EFFECTS OF THRUST VECTORING ON TAKE-OFF AND COMBAT PERFORMANCE

By
Lieut. N. S. GUJRAL, I. N.

DEPARTMENT OF AERONAUTICAL ENGINEERING
INDIAN INSTITUTE OF TECHNOLOGY KANPUR
AUGUST 1973

EFFECTS OF THRUST VECTORING ON TAKE-OFF AND COMBAT PERFORMANCE

A Thesis Submitted
In Partial Fulfilment of the Requirements
for the Degree of
MASTER OF TECHNOLOGY

By
Lieut. N. S. GUJRAL, I. N.

to the

DEPARTMENT OF AERONAUTICAL ENGINEERING
INDIAN INSTITUTE OF TECHNOLOGY KANPUR
AUGUST 1973

ACKNOWLEDGEMENTS

I am indebted to Professor T.M. Kutty for suggesting this interesting topic and for all his guidance, help and encouragement throughout the thesis work.

I am thankful to Mr. C.V.R. Murti for his valuable suggestions and discussions from time to time. Thanks are also due to all my friends for their immense help.

I am grateful to Mr. Kumar for his excellent and patient typing.

N.S. GUJRAL

LIST OF TABLES

LIST OF FIGURES

LIST OF FIGURES (Contd.)

LIST OF FIGURES (Contd.)

LIST OF SYMBOLS

C_L	Conventional list coefficient
C_D	Conventional drag coefficient
C_{D_o}	Parasitic drag coefficient
$C_{L_{LO}}$	Coefficient of lift at lift-off
C_{L_α}	Slopè of C_L - α curve
V	velocity in ft./sec.
V_{LO}	Lift-off velocity
$V_{rot.}$	Velocity at which aircraft rotation on ground begins
α	Conventional angle of attack
α_g	Angle of attack in ground attitude
α_{LO}	Angle of attack at lift-off
α_{ZL}	Zero lift angle of attack
D	Conventional drag
L	Conventional lift
$T_{st.}$	Static thrust at sea level
T	Thrust at a given velocity
T_{LO}	Thrust at lift-off
δ_N	Nozzle inclination with respect to body axis
μ	Surface coefficient of friction
W	Aircraft wieght in lbs
γ	Climb angle
R_H	Total wheel reaction of the aircraft

LIST OF SYMBOLS (Contd.)

T_V	Forward component of thrust i.e. along flight path - lbs
T_L	Component of thrust in the lift direction - lbs
K	Linearity constant for thrust variation with velocity
t	Time in seconds
t_i	Inflexion occurs after so many seconds
t_e	Rotation ends after so many seconds
ρ	Air density lb/ft.^{3}
S	Total wing area ft.^{2}
e	Oswald's efficiency factor
AR	Aspect ratio
m	Total aircraft mass lb-sec^2/ft.
$\dot{V}$	Acceleration ft/sec.^{2}
g	Acceleration due to gravity ft/sec.^{2}
R	Turn radius - ft.
R_{min}	Least radius of turn at constant speed - ft.
ϕ	Bank angle
M	Mach number
η_W	Wing load factor L/W
η_A	(For vectored thrust only). effective aircraft load factor $L+T_L/W$
δ	Inclination of thrust vector to flight path $\delta_N+\alpha$
δt	time increment

LIST OF SYMBOLS (Contd.)

Ψ	Inclination of longitudinal axis of the aircraft with respect to initial direction - radians
$\delta\Psi$	Increment in Ψ due to an increment δt in t
X, Y	Cartesian position co-ordinates of the aircraft with origin at the initial position
δX	Increment in X due to an increment δt in t
δY	Increment in Y due to an increment δt in t.

SYNOPSIS

Vectored thrust V/STOL (Harrier type) performance capabilities are explored in three distinct regimes namely short take-off, constant speed turns and combat turns involving multiple passes over a target.

The strategy for short take-off is to use a single thrust vector inclination (relative to body axis) during the ground roll. The nozzle inclination corresponding to a minimum total lift-off distance is determined for various thrust/weight ratios. Total lift-off distance is the sum of 'ground roll upto rotation and 'Roll during rotation'. The rotation is defined such that the 'Lift-off velocity' is reached at the end of rotation. The reduction in lift-off distance for various T/W ratios is compared with that of conventional take-off. A computer programme has been developed to give 'Optimum nozzle angle' for take-off

a) for minimum lift-off distance

and b) for minimum time.

It is found that an optimum nozzle angle exists for each T/W ratio to give least ground distance for lift-off but the advantage over conventional take-off is substantial down to T/W ratio of approximately 0.4. Below 0.4 the advantage is not much significant.

For analysis of constant speed turns a computer programme is developed to calculate least radius constant speed turning performance using vectored thrust. The turning performance of conventional configuration is also calculated for comparison. The programme takes into account C_{Lmax} variation with Mach number and the limiting load factors.

For analysing combat turn performance where speed can vary, a programme is developed for the case where a vectored thrust aircraft enters a turn at a given initial velocity and progressively reduces the speed and therefore the radius of turn to come back to the target i.e. the initial point of entry into the turn for a second pass.

CHAPTER I

INTRODUCTION

From the first short hops by Wright brothers upto the present day hypersonic flight, advances in aeronautics have usually been associated with increase in speed. Speed and more speed has been a primary objective but since last few years in addition to emphasis on the maximum speed, there has been an interest to achieve better low speed performance. In attempting to achieve high maximum speeds the conventional configuration has to pay a penalty in terms of higher take-off speed and distance and in addition the manoeuvrability is also drastically reduced in terms of the turning radius. Thrust vectoring not only permits a vertical/short take-off but also improves combat manoeuvre performance significantly. It also tends to give the pilot more margin or flexibility in three distinct regions of flight namely take-off, landing and manoeuvres.

This report explores the capabilities of thrust vectoring for V/STOL jet aircraft in as much as short take-off, constant speed turns and combat turns are concerned and shows a clear edge over conventional aircraft in these regimes.

Since the only aircraft in the world today using thrust vectoring and having attained the operational status is 'Harrier' seeing active squadron service with RAF and USMC and after having logged thousands of flying hours has conclusively proved the

simplicity and practicability of single engine thrust vectoring formula, as such the aircraft constants used in the simulated aircraft of this report are those of Harrier.

Full potential of thrust vectoring cannot be achieved in the present state of art due to aircraft limitations i.e. how far the nozzles may be swivelled at various air speeds? For example, Harrier power is limited to 80% if ducts are swivelled through their full range between 250-300 knots IAS and between 300-400 knots IAS, nozzle travel is limited to 45° only in addition to 80% power limitation. Nevertheless modifications are under current evaluations to eliminate these restrictions and no such restrictions have been imposed on the simulated aircraft of this report.

It may well be mentioned here that thrust vectoring has not yet been used for manoeuvrability in practice but up-to-date research and simulated studies indicate that greatest change by thrust vectoring will be brought in air to air combat role because vectored thrust assisted manoeuvrability would vastly increase the turning capability. This report confirms this opinion.

It may be of interest to note the type of work presently being carried out in the field of thrust vectoring. Current research includes NASA working on predecessor 'KESTREL' for study of manoeuvrability by vectored thrust. USAF is also doing

same objective and studies on same lines are also being carried out by Institute of Defence analysis. A combined NASA + U.K., 3 phase programme has already been finalised for Harrier. Since there is 80% power limitation between 200-300 knots in current Harrier, phase one will try to expand " Inflight vectoring envelope" to 500 knots. Flight work is to be preceded by wind tunnel work in Britain and work in DMS (Dual Manoeuvring Simulator) on air to air combat with usual guidance by NASA. Phase two will aim to expand inflight vectoring envelope to maximum which will be in excess of 600 knots and slightly less than 100% power. Phase three is a long term process - 3 to 4 years. In order to move the nozzles at high aerodynamic loads encountered at greater airspeeds, nozzles will be aerodynamically balanced instead of increasing drive system power. In this phase NASA has planned to

1. study wing geometry variations to optimise the wing for thrust vectored assisted manoeuvrability.

2. study effects of stability augmentation system on thrust vectored aircraft in regards to problems like 'deep stall' etc.

3. study various interconnections between aerodynamic controls and thrust vectoring and control system i.e. method of interconnecting thrust vectoring system with aerodynamic tail surfaces to counteract pitching problems which can be experienced during nozzle movements.

4. design new special tunnels for V/STOL aircrafts to be installed by 1980 with a view to bring about a cut in V/STOL programme costs.

CHAPTER II

TAKE-OFF PERFORMANCE

2.1 Minimum Lift-off Distance for Vectored Thrust Aircraft:

The question to be considered is the following - starting with the aircraft with 'BRAKES ON', how should the controls be operated and the 'ground roll' and 'rotation' chosen, in order to lift the aircraft 'off' the ground in an optimum fashion. Optimum can mean different things at different times but in this context it usually means the minimum lift-off distance for a given aircraft configuration.

2.1.1 Method of analysis

The optimum scheme is as outlined below. As shown in Figure 1 the aircraft gathers speed from stage I to stage II in ground attitude. After it has attained a certain desired velocity (termed hereafter as $V_{rot.}$), the aircraft incidence is gradually increased in a predetermined manner (i.e. rate of rotation and incidence pattern are specified). It is desired that at the end of rotation the velocity attained should compare with the aircraft lift-off velocity. Thus the problem remains to decide upon the instant at which the rotation must start or in other words what should $V_{rot.}$ be? A programme has been developed to fit into above scheme which makes use of an iterative procedure to arrive at the exact value of $V_{rot.}$ Flow

chart and the programme listing appear in Appendix-A. Following are the assumptions on which the subsequent analysis is based.

(i) For ground roll upto rotation, drag, lift and thrust are functions of velocity.

(ii) For roll during rotation, lift coefficient and drag coefficient are functions of angle of attack together with the assumption (i).

(iii) Parabolic drag polar is assumed.

(iv) Aircraft weight does not alter on account of fuel being consumed and effects of changes in ambient temperature are neglected.

For vectored thrust short take-off, two operational methods can be conceived of namely

a) to use a single thrust vector inclination (relative to body axis) during the ground roll and initial climbout (air phase portion of take-off) and the inclination chosen would correspond to a minimum ground distance.

or b) to point the thrust vector in horizontal direction during the ground roll and then to rotate the thrust vector instantaneously to optimum angle for initial climb-out (air-phase).

Air-phase horizontal distance is same for cases a) and b) but ground roll is shorter for case b) due to higher horizontal acceleration whereas the list-off speed is same for both

but however case b) is difficult to achieve in practice and as such in present analysis method a) has been preferred.

Aircraft constants used for simulation are close to Harrier and appear in Table - 1 and $C_L - \alpha$ curve used is shown in Figure 4. Lift curve shows a slope of 5 per radian together with a zero lift angle of attack of -5 degrees. Lift-off angle of attack is 8 degrees.

Specified rate and pattern of rotation are as indicated in Figure 3. To start with, let us assume a 4th order poly nomial

$$\alpha = a + bt + ct^2 + dt^3 + et^4 \qquad (1)$$

where a, b, c, d, e are some constants.

Boundary conditions are i) $t = o, \quad \alpha = \alpha_g, \quad \frac{d\alpha}{dt} = 0$

ii) $t = t_i, \quad \frac{d^2\alpha}{dt^2} = 0$

iii) $t = t_e, \quad \alpha = \alpha_{LO}, \quad \frac{d\alpha}{dt} = 0$

where t_e = rotation ends after so many seconds

t_i = inflexion starts after so many seconds.

By using these boundary conditions, we arrive at the set of following equations:

$$a = \alpha_g \qquad (2)$$

$$b = 0 \qquad (3)$$

$$\alpha_{LO} = \alpha_g + c\, t_e^2 + d\, t_e^3 + e\, t_e^4 \qquad (4)$$

$$0 = 2c\ t_e + 3d\ t_c^2 + 4e\ t_e^3 \qquad (5)$$

$$0 = 2c + 6d\ t_i + 12\ e\ t_i^2 \qquad (6)$$

simultaneous solution of (5) and (6) gives

$$d|\ 3t_e - 6t_i\ | + e\ |\ 4t_e^2 - 12t_i^2\ | = 0 \qquad (7)$$

similarly (4) and 6) yield

$$d|\ t_e - 3t_i\ | + e\ |\ t_e^2 - 6t_i^2\ | = \frac{\alpha_{LO}-\alpha_g}{t_e^2} \qquad (8)$$

(7) and (8) simultaneously yield

$$e = (\alpha_{LO}-\alpha_g)\ (3t_e-6t_i)/t_e^3(6t_e\ t_i-6t_i^2-t_e^2)$$

$$d = 4(\alpha_{LO}-\alpha_g)(3t_i^2-t_e^2)/t_e^3(6t_e t_i-6t_i^2-t_e^2)$$

substitution of values of e and d in (6) yields

$$c = 6t_i(\alpha_{LO}-\alpha_g)(2t_e-3t_i)/t_e^2(6t_e\ t_i-6t_i^2-t_e^2)$$

Redesignating constants c, d, e as A, B, C (in agreement with the programme listing) we arrive at

$$\alpha = \alpha_g + At^2 + Bt^3 + Ct^4 \qquad (9)$$

are determined from known input values of t_e, t_i, α_{LO}, α_g

2.1.2. Equations of motion:

We consider a general vectored thrust configuration (Figure 2) having only propulsive jet engine whose thrust can

be vectored.

T denotes the installed thrust of the propulsive engine and δ_N represents the angle of rotation of the thrust vector relative to the aircraft body axis. A linear velocity dependence is assumed for thrust i.e. $T = T_{st.} - KV$ where K is a constant.

$$\text{Total wheel reaction } R_H = \mu \mid W - L - T_L \mid \qquad (10)$$

<u>during round roll</u> : $\alpha = \alpha_g = \text{constant}$

$$\text{and } T_V = T \cos(\alpha_g + \delta_N) \qquad (11)$$

$$T_L = T \sin(\alpha_g + \delta_N) \qquad (12)$$

$$L = \frac{1}{2} \rho S V^2 C_L = \frac{1}{2} \rho S C_{L_\alpha} \alpha_g V^2 = C_1 V^2$$

$$D = \frac{1}{2} S V^2 C_D = \frac{1}{2} \rho S (C_{D_o} + C_{L_\alpha}^2 \alpha_g^2 / \pi e AR) V^2 = C_2 V^2$$

where $C_1 = \frac{1}{2} \rho S C_{L_\alpha} \alpha_g$

$$C_2 = \frac{1}{2} \rho S (C_{D_o} + C_{L_\alpha}^2 \alpha_g^2 / \pi e AR)$$

Summation of forces along the flight path gives

$$m\dot{V} = T_V - D - \mu(W - L - T_L) \qquad (13)$$

substituting the values for T_V, D, L, T_L we get

$$\dot{V} = \frac{g}{W} \mid T_{st.} \cos(\delta_N + \alpha_g) - \mu W + \mu T_{st.} \sin(\delta_N + \alpha_g) \mid$$

$$- \frac{g}{W} \mid C_2 - \mu C_1 \mid V^2 - \frac{g}{W} \mid K \cos(\delta_N + \alpha_g) + \mu K \sin(\delta_N + \alpha_g) \mid V$$

$$= C_{10} - C_{11} V - C_{12} V^2 \qquad (14)$$

where

$$C_{10} = (g/W) \mid T_{st.} \cos(\delta_N + \alpha_g) + \mu \sin(\delta_N + \alpha_g) \mid - \mu W$$

$$C_{11} = K \mid \cos(\delta_N + \alpha_g) + \mu \sin(\delta_N + \alpha_g) \mid g/W$$

$$C_{12} = (C_2 - \mu C_1)\, g/W$$

<u>during rotation:</u>

α is variable and $T_V = T \cos(\alpha + \delta_N)$ (15)

$$T_L = T \sin(\alpha + \delta_N) \qquad (16)$$

$$L = \frac{1}{2} \rho S V^2 C_L = \frac{1}{2} \rho S C_{L_\alpha} \alpha V^2 = C_3 \alpha V^2$$

$$D = \frac{1}{2} \rho S V^2 \left(C_{D_o} + \frac{C_L^2}{\pi e AR}\right) = \frac{1}{2} \rho S V^2 \left| C_{D_o} + C_{L_\alpha}^2 \alpha^2 / \pi e AR \right|$$

$$= C_4 V^2 + C_5 \alpha^2 V^2$$

where

$$C_3 = \frac{1}{2} \rho S C_{L_\alpha}$$

$$C_4 = \frac{1}{2} \rho S C_{D_o}$$

$$C_5 = \frac{1}{2} \rho S C_{L_\alpha}^2 / \pi e AR$$

Thus once again using the values for T_V, D, L, T_L in the equation for $m\dot{V}$ we arrive at

$$\dot{V} = (g/W) \mid T_{st.} \cos(\delta_N + \alpha) - \mu W + T_{st.} \mu \sin(\delta_N + \alpha) \mid$$

$$- (g/W) C_4 V^2 - (g/W) \mid K \cos(\delta_N + \alpha) + \mu K \sin(\delta_N + \alpha) \mid V$$

$$+ (g/W) \mu C_3 \alpha V^2 - (g/W) C_5 \alpha^2 V^2$$

$$= (g/W) \left| T_{st.} \cos(\delta_N+\alpha) + \mu \sin(\delta_N+\alpha) - \mu W \right| -$$

$$- \left(\frac{gK}{W}\right) \left| \cos(\delta_N+\alpha) + \mu \sin(\delta_N+\alpha) \right| V + \left| C_{13}\alpha - C_{14}\alpha^2 - C_{15} \right| V^2 \qquad (17)$$

where

$$C_{13} = (g/W)\ \mu C_3$$

$$C_{14} = (g/W)\ C_5$$

$$C_{15} = (g/W)\ C_4$$

2.2 Lift-off Velocity :

Vertical equilibrium at lift-off is assumed so that

$$W = C_{L_{LO}} \frac{\rho}{2} V_{LO}^2 S + T_{LO} \sin(\delta_N + \alpha_{LO}) \qquad (18)$$

where $T_{LO} = T_{st.} - K V_{LO}$ substituting this we obtain a quadratic in V i.e.

$$V_{LO}^2 (S \rho C_{L_{LO}}) - 2K \sin(\delta_N+\alpha_{LO})\ V_{LO} + \left| 2 T_{st.} \sin(\delta_N+\alpha_{LO}) - 2W \right| = 0 \qquad (19)$$

which yields

$$V_{LO} = \frac{2K \sin(\delta_N+\alpha_{LO}) \pm \sqrt{4K^2 \sin^2(\delta_N+\alpha_{LO}) - 4 S \rho C_{L_{LO}} \left| 2T_{st.} \sin(\delta_N+\alpha_{LO}) - \right.}}{2 S \rho C_{L_{LO}}}$$

since our analysis is continued to the case W > T always and hence the positive sign to be used.

denoting ARG = $\delta_N + \alpha_{LO}$, we have

$$V_{LO} = K \sin(ARG) + \sqrt{K^2 \sin^2(ARG) - 2S\rho C_{L_{LO}} |T_{st.} \sin(ARG) - W|} \Big/ S\rho C_{L_{LO}}$$

where α_{LO} and $C_{L_{LO}}$ are specified inputs.

2.3. Results and Discussions:

Nozzle angle is varied from 0° to 80° in steps of 1° and lift-off distance, lift-off time and lift-off velocity is calculated for various aircraft weights. It is seen that for a given aircraft configuration there are particular nozzle angles for which, time and distance to lift-off is a minimum. Figures 9 and 10 show these minima for a thrust/weight ratio of 0.5 and Figures 7 and 8 show these minima for a thrust/weight ratio of 0.95.

It is seen that for a given configuration the nozzle angles corresponding to minimum time can differ considerably from those for minimum distance. Lift-off velocity drops with increasing nozzle angles and the gradient steepens as thrust/weight ratio increases. Figure 11 shows lift-off velocity v/s nozzle angles for thrust/weight ratio of 0.5 and 0.95.

For minimum lift-off distance case - Table 3 presents the effect of variation in weight on optimum nozzle angle, lift-off velocity and distance to lift-off.

For the case of minimum lift-off time - Table 4 presents the effect of variation in weight on optimum nozzle angle and time to lift-off.

Figure 12 presents the plots for optimum nozzle angles for various aircraft weights. Curve (1) corresponds to minimum lift-off distance and curve (2) corresponds to minimum lift-off time.

The reductions in lift-off distance, lift-off time and lift-off velocities for various aircraft weights over that of conventional configuration are presented in Figures 13, 14 and 15 respectively.

It is seen that these reductions are not much significant for thrust weight ratios less than about 0.4. However, for higher T/W ratios the reductions are substantial. For example at T/W ratio of approximately .95 the reductions in lift-off distance, lift-off time and lift-off velocity are of the order of 35%., 20%. and 70%. respectively whereas for a T/W ratio of .5 they are 10%., 3%. and 11%. respectively.

CHAPTER III

COMBAT PERFORMANCE: CONSTANT SPEED TURNS

It will be shown in this chapter that more tighter 'minimum radius constant speed turns' can be obtained by vectoring the thrust.

'Constant altitude co-ordinated turn' only is considered i.e. pure rotation of the aircraft about a fixed axis in the atmosphere (generalised turn problem wherein aircraft changes both its azimuth heading as well as the inclination of its flight path to the horizontal can be further undertaken). In a co-ordinated turn, aircraft may be pitched with respect to the flight path but it may not be yawed i.e. a slipping or skidding turn cannot be considered a coordinated turn. Condition for co-ordinated turn is that a plane passed through the longitudinal (X) axis of the aircraft which includes the aircraft's vertical axis (Z) must also include the tangent to the flight path passing through the airplane's centre of gravity. Under these conditions 'ONLY' one aircraft is not yawed and is in a coordinated turn.

Turning radius becomes a minimum when the aircraft is at the stalling angle of attack and since the velocity in constant altitude flight is limited by the available thrust and hence the maximum value of bank angle is limited. Thus constant altitude co-ordinated turn radius is limited by

(i) Stalling angle of attack i.e. C_{Lmax} limit.

(ii) By thrust available i.e. thrust limit.

(iii) Since C_{Lmax} is a function of Mach number, another speed restriction is imposed on minimum turn radius by aircraft's inability to fly at a high angle of attack at high speeds.

If constant altitude restriction for turn is not there and if can permit climb or decent during the turn.- a somewhat smaller turning radius may be obtained but this case is not considered here.

Constant speed is maintained by scheduling the thrust vectoring in such a way that the component of thrust along the flight path just balances the drag and thus arrests any deceleration which might be caused due to banking. Thus theoretically there exists an optimum nozzle angle for minimum radius turn at each speed.

During the manoeuvre, the wing and the aircraft load factors defined as $\eta_W = L/W$ and $\eta_A = \frac{L+T_L}{W}$ are not to exceed maximum permissible values.

C_{Lmax} variation with Mach number for the simulated aircraft of this report is shown in Figure 16 wherein upto a Mach number of 0.5, $C_{L_{max}}$ remains constant at a value of 1.0 and gradually drops to a value of 0.4 when Mach number of the order of 0.9 is reached.

Analysis:

Expressions for turn radius in terms of turn velocity are obtained by considering the equilibrium of forces as shown in Figure 17 and by considering the optimum condition of Figure 18.

From equilibrium of forces, we obtain

$$(L + T_L) \cos \phi = W \tag{1}$$

$$(L + T_L) \sin \phi = \frac{W}{g} \frac{V^2}{R} \tag{2}$$

which are rewritten as

$$\phi = \cos^{-1} \frac{W}{L + T_L} \tag{3}$$

$$R = \frac{W/g\ V^2}{(L + T_L) \sin \phi} \tag{4}$$

substituting for ϕ from (3) into equation (4) we obtain

$$R = \frac{W/g\ V^2}{(L + T_L) \sin \left| \cos^{-1} \frac{W}{L + T_L} \right|} \tag{5}$$

for minimum radius at constant speed we use $L = \frac{1}{2} \rho V^2 S C_{L_{max}}$ provided L/W does not exceed $(\eta_W)_{max}$, if it does then the C_L value is modified to $C_L = (\eta_W)_{max}\ W/\frac{1}{2} \rho V^2 S$ and also it is checked that $\frac{L+T_L}{W}$ does not exceed $(\eta_A)_{max}$, if it does, the T_L value is modified to $T_L = (\eta_A)_{max} W - L$. The expression for T_L is obtained from the optimum conditions of Figure 18 which gives

$$T_L = T \sin \delta \qquad (6)$$

$$T_V = T \cos \delta \qquad (7)$$

where $\delta = \delta_N + \alpha$ from which we have $\delta = \cos^{-1} \frac{T_V}{T}$ (8)

and $$T_L = T \sin (\cos^{-1} \frac{T_V}{T}) \qquad (9)$$

where $$T_V = D = \frac{1}{2} \rho V^2 S (C_{D_o} + \frac{C_L^2}{\pi e R}) \qquad (10)$$

The final expression for minimum radius becomes

$$R_{min} = \frac{W/g \; V^2}{|T \sin(\cos^{-1} \frac{T_V}{T}) + L| \sin(\cos^{-1} \frac{W}{T \sin(\cos^{-1} \frac{T_V}{T}) + L})}$$

The conventional case is derived from above by using $T_L = 0$.

The programme listing which takes into account the $C_{L_{max}}$ variation with Mach number and load factor limitations and evaluates minimum radius constant speed turns for conventional as well as vectored thrust aircraft for any combination of thrust, weight and altitude is appended at Appendix B.

Results and Discussions:

Results are presented in Figures 19 to 26 covering both sea level and altitude (20,000') conditions for a range of thrust-weight ratios varying from 0.5 to 1.0. Following trends are observed:

(i) The minimum radius decreases both at sea level and altitude with speed. As speed reduces C_{Lmax} is proportionately higher down to a Mach number of 0.5 below which the C_{Lmax} is constant. However, limitation in C_L can also be experienced due to limiting load factor. Thus with reducing speed the minimum radius falls steeply till the aircraft encounters limiting load factor or till the Mach number below which C_{Lmax} is constant is reached. Thereafter the gradient is less steep in case of thrust vectoring whereas the curve starts rising for conventional aircraft. The comparison ends with the conventional aircraft reaching stalling speed.

(ii) For a given speed minimum radius is higher at altitudes.

(iii) Percentage reduction in minimum radius by thrust vectoring is maximum at speeds approaching stalling speed and is quite substantial (i.e. at sea level it is of the order of 30% and 50% for thrust/weight ratio of 0.5 and 1.0 respectively For speeds approaching maximum speed the percentage reductions are much less pronounced (i.e. at sea level they are of the order of 5% and 18% for thrust/weight ratio of 0.5 and 1.0 respectively).

CHAPTER IV

COMBAT PERFORMANCE: OPTIMUM TURNS

This chapter analyses a combat turn, where the speed can vary and it is shown that thrust vectoring can also be used for added 'combat manoeuvrability' coupled with superior turning performance in terms of the time saved in making a full turn to come back to the target by thrust vectoring over that of conventional. The use is made of the fact that the turn radius falls with speed.

The conventional as well as vectored thrust aircraft enter a turn with the same known initial velocity. The conventional aircraft decelerates by cutting down its thrust whereas the vectored thrust aircraft decelerates by completely cutting off T_V (thrust component along the flight-path) by swivelling the nozzles fully downwards through 90 degrees, thus making it possible for the aircrafts to turn tighter and tighter progressively. Following is borne in mind during the entire manoeuvre

(1) Load factors should not exceed the maximum specified limits.

(2) Aircrafts are to keep well above stall velocity while decelerating and as stalling speed approaches further deceleration is arrested by continuing with constant radium steady turn by swivelling the nozzles back to an angle decided by $T_V = D$ and in case of conventional aircraft by increasing the thrust.

(3) Turn is continued till the aircrafts are in line with the target (initial point of entry into the turn) again. Once this is achieved the aircrafts level up and accelerate with full throttle towards the target (vectored aircraft having swivelled its nozzles fully back to horizontal).

Based on above strategy a computer programme is developed which calculates the time to come back to the initial point of entry into the turn for a second pass and compares it with the conventional case for any combination of initial velocity, thrust weight ratio and altitude and gives aircraft position co-ordinates with respect to the initial point of entry into the turn. The Flow Chart and programme listing appear in Appendix 'C'.

Analysis:

Since at the commencement of the turn forward component of thrust is cut-off (i.e. $T_V = 0$) as such the force diagram is as it appears in Figure 27. From equilibrium of forces we obtain

$$(L+T) \sin \phi = \frac{W}{g} \frac{V^2}{R} \quad \text{where } \phi = \sin \left(\cos^{-1} \frac{W}{L+T}\right)$$

Hence
$$R = \frac{W/g \; V^2}{(L+T) \sin\left(\cos^{-1} \frac{W}{L+T}\right)}$$

Since minimum radius is at stalling angle of attack we use $L = 1/2 \rho V^2 S C_{L_{max}}$ as long as $\frac{L}{W} \not> (\eta_W)_{max}$. If it does

exceed C_L value is modified to $\frac{(\eta_W)_{max.}\ W}{\frac{1}{2}\rho V^2 S}$ and also $\frac{L+T}{W}$ is not to exceed $(\eta_A)_{max}$, in case it exceeds, the thrust is throttled back to adjust to $T = (\eta_A)_{max.}$ W-L. Thus having decided upon C_L value the drag is calculated by using the expression $D = 1/2\ \rho V^2 S\ (C_{D_o} + \frac{C_L^2}{\pi e R})$ which gives the deceleration $\dot{V} = -D/(W/g)$.

By choosing time as independent parameter and taking the aircraft longitudinal axis as the reference axis for measuring the angle through which the aircraft is turning we have (see Figure 28).

$$\delta\Psi = V\ \delta t/R$$

$$\delta Y = V\ \delta t \sin \Psi$$

$$\delta X = V\ \delta t \cos \Psi$$

where V and R vary from instant to instant.

The condition for the aircraft to be in line with the target (initial point of entry) is

$$\tan \Psi = \frac{Y}{X}$$

where Y and X are the cartesian co-ordinates of the aircraft position with respect to the origin at initial point of entry. Once this is attained the aircraft levels up and speeds straight ahead with an acceleration given by T-D/(W/g).

Results and Discussion:

Based on above strategy, the flight trajectory plots of conventional and vectored thrust aircraft have been presented in Figure 29 to Figure 36, both for sea level and altitude, for a range of thrust-weight ratios from 0.5 to 1.0.

The percentage saving in time in each case by thrust vectoring is compiled in Table 6. It is assumed that the aircraft enters the turn in each case at a Mach number of 0.8.

It is observed that percentage saving in time is of the order of 16%., 17%. and 24%. for thrust/weight ratios of 0.5, 0.8 and 1.0 respectively at sea level and 31%., 21%., 19%. respectively at altitude of 20,000'.

Decelerations observed have been of the order of -.25g-.3g and much better results could be expected if higher deceleration rates can be achieved in some way or the other, for example by reversing the nozzles since decelerations of -0.45g to -0.5g are known to be quite comfortable for fighter pilots.

An interesting case of a study by NASA on its Dual Manoeuvring Simulator (D.M.S. - commissioned in 1968) is presented in Figure 37. It is, however, not known what techniques were used for achieving higher decelerations for vectored thrust aircraft. Nevertheless it is seen that after eleven seconds

the speed of vectored thrust aircraft has reduced from Mach 1.0 to 0.4 and turn radius from 4000' to 2500' and instantaneous turn reversal has been achieved which brings it behind the conventional aircraft which still is travelling at Mach 0.8 and a turn radius of near about 4000', thus concluding that thrust vectoring can uniquely be used in converting an 'attacked' role to an 'attacker' role by using rapid deceleration capability. To further drive home this claim three possible combat encounters studied on NASA's D.M.S. are shown in Figures 38, 39 and 40, which show relative turn superiority of vectored thrust over conventional.

Figure 38 depicts case of a vector-thurst aircraft being attacked from behind and Figure 39 depicts them in reversed roles. Figure 40 depicts how vectored-thurst superiority can be taken advantage of in head-on combat.

CHAPTER V

CONCLUSIONS

It is concluded that thrust vectoring has a clear edge over conventional aircraft in so far as take-off performance, constant speed turns and combat turns are concerned.

It is found that an optimum nozzle angle exists for each thrust/weight ratio to give minimum lift-off distance and the reduction is substantial for thrust/weight ratio greater than about 0.4.

Constant speed minimum turn radius is substantially reduced by thrust vectoring both at sea level and altitudes.

Substantial gain over conventional aircraft in terms of time saved to make a second pass over a target can be achieved by thrust vectoring.

It is seen that greatest advantage of thrust vectoring would be in air to air combat role and use of thrust vectoring for combat role may not be difficult to adopt since pulling back on the thrust vector control, in effect, is same as pulling back on control stick and if by proper vector scheduling, turn radius can be made independent of aircraft speed and if more deceleration rates can be attained by nozzle reversals, thrust vectoring may even prove more promising.

TABLE 1

AIRCRAFT CONSTANTS

Wing Area	S	200 ft^2
Aspect Ratio	AR	3.2
Sea level Static Thrust	T	19000 lbs
Efficiency Factor	e	0.7
Drag Coefficient (Parasitic)	C_{D_o}	0.02
Friction Coefficient	μ	0.03
Ground Incidence	α_g	1.0 deg.
Lift Curve Slope	C_{L_α}	5 per radian
Zero lift angle of attack	α_{ZL}	- 5.0 deg.
Lift off angle of attack	α_{LO}	8.0 deg.
Period of Rotation	t_{rot}	3 seconds
Inflexion Ratio		2:1

TABLE 2

TAKE-OFF-PERFORMANCE

Nozzle angle δ_N deg.	Total lift-off distance in ft.		List of velocity in fps		Time to lift-off in sec.	
	T/W =0.95	T/W = 0.5	T/W=0.95	T/W=0.5	T/W=0.95	T/W=0.
1.	2.	3.	4.	5.	6.	7.
0	1353	5206	272	375	9.7	26.9
1	1343	5170				
2	1326	5133				
3	1310	5095				
4	1298	5062				
5	1271	5028	262	368	9.4	26.5
6	1259	5000				
7	1231	4963				
8	1218	4940				
9	1190	4907				
10	1177	4881	251	361	9.1	26.2
11	1164	4853				
12	1140	4831				
13	1127	4808				
14	1103	4790				
15	1094	4763	240	354	8.9	26.1
16	1070	4743				
17	1055	4728				
18	1045	4711				

TABLE 2 (Contd.)

1.	2.	3.	4.	5.	6.	7.
19	1021	4693				
20	1011	4680	228	346	8.6	26.2
21	991	4666				
22	976	4650				
23	965	4639				
24	945	4633				
25	933	4626	216	339	8.4	26.5
26	922	4617				
27	910	4612				
28	890	4606				
29	878	4605				
30	865	4601	204	332	8.3	27
31	853	4603				
32	836	4608				
33	824	4611				
34	815	4612				
35	802	4624	191	324	8.2	27.8
36	792	4633				
37	779	4691				
38	769	4707				
39	751	4729				
40	740	4743	178	318	8.1	29.2

TABLE 2 (Contd.)

1.	2.	3.	4.	5.	6.	7.
41	731	4762				
42	720	4835				
43	709	4860				
44	698	4893				
45	686	4923	165	311	8.1	30.9
46	675	4960				
47	666	5049				
48	654	5095				
49	644	5143				
50	635	5251	152	305	8.2	33.6
51	622	5305				
52	612	5371				
53	601	5441				
54	593	5570				
55	582	5655	139	299	8.3	36.9
56	573	5742				
57	564	5903				
58	555	6012				
59	544	6192				
60	534	6323	126	294	8.5	42.0

TABLE 2 (Contd.)

1.	2.	3.	4.	5.	6.	7.
61	530	6463				
62	521	6688				
63	518	6850				
64	514	7052				
65	507	7333	114	290	9.0	49.4
66	506	7565				
67	505	7908				
60	504	8194				
69	503	8611				
70	502	8977	102	286	9.9	61.4
71	507	9493				
72	508	9966				
73	514					
74	523					
75	532		91	282	11.7	82.9
76	546					
77	560					
78	580					
79	610					
80	647		83		15.8	

TABLE 3

TAKE-OFF PERFORMANCE

Weight lbs	Optimum nozzle angle for least L.O. distance degrees	Total L.O. distance ft.	Total L.O. with δ_N=0 ft.	δ_N=opt. $V_{rot.}$ fps	δ_N=opt. L.O. vel. fps	δ_N = 0 $V_{rot.}$ fps	δ_N = 0 L.O. vel. fps
1.	2.	3.	4.	5.	6.	7.	8.
19500.	73.0	375.	1294.	55	83	188.	269.
20000.	69.0	502.	1353.	72	104	193.	272.
20500.	66.0	608.	1423	85.	120.	198.	276.
21000	63.0	708.	1494.	96.	135	294.	279.
21500	61.0	804.	1599.	107	146.	200	282.
22000	57.0	899.	1647	118	161	214	285.
22500	55.0	991.	1730.	127	171.	219	289.
23000	54.0	1082.	1814.	135	179.	225	292.
23500	52.0	1177.	1886.	144.	188.	229	295.
24000	50.0	1279.	1982.	153	197	234	298.
24500	49.0	1365.	2103.	161	204	239	301
25000	48.0	1466.	2164.	169	211	244	304
25500	47.0	1557.	2249.	176	217	248	307
26000	45.0	1657.	2335.	182	227	252	310
26500	44.0	1760	2427.	188	235.	256	313

TABLE 3 (Contd.)

1.	2.	3.	4.	5.	6.	7.	8.
27000	43.0	1862.	2519	194	237	261	316
27500	43.0	1960.	2618.	200	241	265	319
28000	41.0	2067.	2719.	204	248.	268	322.
28500	40.0	21.74	28.50.	209	254.	272	325.
29000	39.0	2283.	2957.	213	259.	276	328.
29500	39.0	2419.	3071.	218	261.	280	331.
30000	39.0	2508.	3152.	223	265.	285	333.
30500	38.0	2644.	3266.	229	270.	289	336.
31000	38.0	2740.	3368.	234	276	292	339.
31500	37.0	2863.	3518.	240	281	296	342.
32000	37.0	2991.	3606.	245	284	300	344.
32500	36.0	3124.	3778.	250	289	305	347.
33000	35.0	3259.	3915.	255	294	309	350.
33500	35.0	3362.	4061.	260.	297	312	352.
34000	34.0	3505	4164.	265	302	315	355.
34500	33.0	3651	4390	271	306	318	358
35000	33.0	3763	4427	274.	309	321	360.
35500	32.0	3917	4576	279.	314	325.	363.
36000	32.0	4032	4687	282.	317	327	365.
36500	31.0	4191	4850	286	320	331	368.
37000	31.0	4311	4968	290	324	333	370.
37500	30.0	4477	5087	296	329	335	373.
38000	30.0	4601	5206	298	332	338	375.

TABLE 4

TAKE-OFF PERFORMANCE

Weight lbs.	Optimum nozzle angle δ_N for least lift-off time degrees	Lift-off time-least sec.	Lift-off time for δ_N=0 sec.
1.	2.	3.	4.
19500	50.0	7.6	9.4
20000	45.0	8.1	9.7
20500	41.0	8.6	10.1
21000	37.0	9.1	10.5
21500	35.0	9.5	11.0
22000	33.0	10.0	11.3
22500	31.0	10.4	11.7
23000	29.0	10.9	12.1
23500	28.0	11.3	12.5
24000	27.0	11.8	13.0
24500	26.0	12.2	13.4
25000	25.0	12.7	13.9
25500	25.0	13.1	14.3
26000	24.0	13.6	14.8
26500	23.0	14.0	15.2
27000	22.0	14.5	15.7
27500	22.0	14.9	16.1
28000	21.0	15.4	16.6
28500	21.0	15.8	17.1

TABLE 4 (Cont'd.)

1.	2.	3.	4.
29000	20.0	16.3	17.6
29500	19.0	16.7	18.1
30000	19.0	17.2	18.6
30500	18.0	17.6	19.1
31000	18.0	18.1	19.6
31500	17.0	18.7	20.2
32000	17.0	19.3	20.7
32500	16.0	19.9	21.2
33000	16.0	20.5	21.7
33500	15.0	21.1	22.2
34000	15.0	21.7	22.7
34500	15.0	22.3	23.3
35000	14.0	22.8	23.7
35500	14.0	23.4	24.3
36000	14.0	23.8	24.8
36500	13.0	24.5	25.4
37000	13.0	25.0	25.9
37500	13.0	25.6	26.4
38000	13.0	26.0	26.9

TABLE 5

a_o = 1116.4 ft/sec.

ρ_o = .002377 lb.sec.^{2}/ft.^{4}

p_o = 2116.2 lb./ft.^{2}

Altitude ft.	Sound velocity ratio SVR = $\frac{a}{a_o}$	Air density ratio $\frac{\rho}{\rho_o}$	Pressure PR = $\frac{p}{p_o}$
0	1	1	1
10,000	.9650	.7385	.6877
20,000	.9287	.5328	.4595
30,000	.8909	.3741	.2970
40,000	.8671	.2971	.2234

TABLE 6

COMBAT PERFORMANCES: OPTIMUM TURNS

Thrust/weight = 1.0	Initial Entry Mach No.	Time to come back to the target-seconds SEA LEVEL		Altitude-20,000'	
		Vectored	Conventional	Vectored	Conventional
Thrust/weight =0.8	0.8	53.0	63.0	137.4	201.1
Thrust/weight =0.8	0.8	40.7	49.2	68.7	87
Thrust/weight =0.5	0.8	38.0	50.0	52.9	65.3

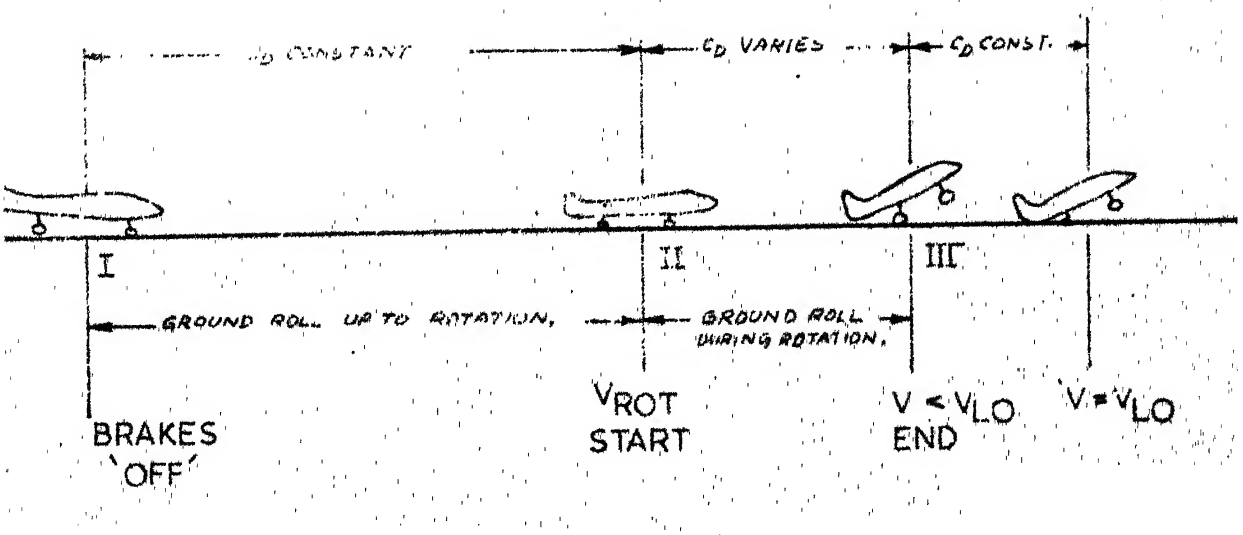
C_D CONSTANT
C_D VARIES
C_D CONST.
I
II
III
GROUND ROLL UP TO ROTATION,
GROUND ROLL DURING ROTATION,
BRAKES 'OFF'
V_{ROT} START
$V < V_{LO}$ END
$V = V_{LO}$

FIG. 1

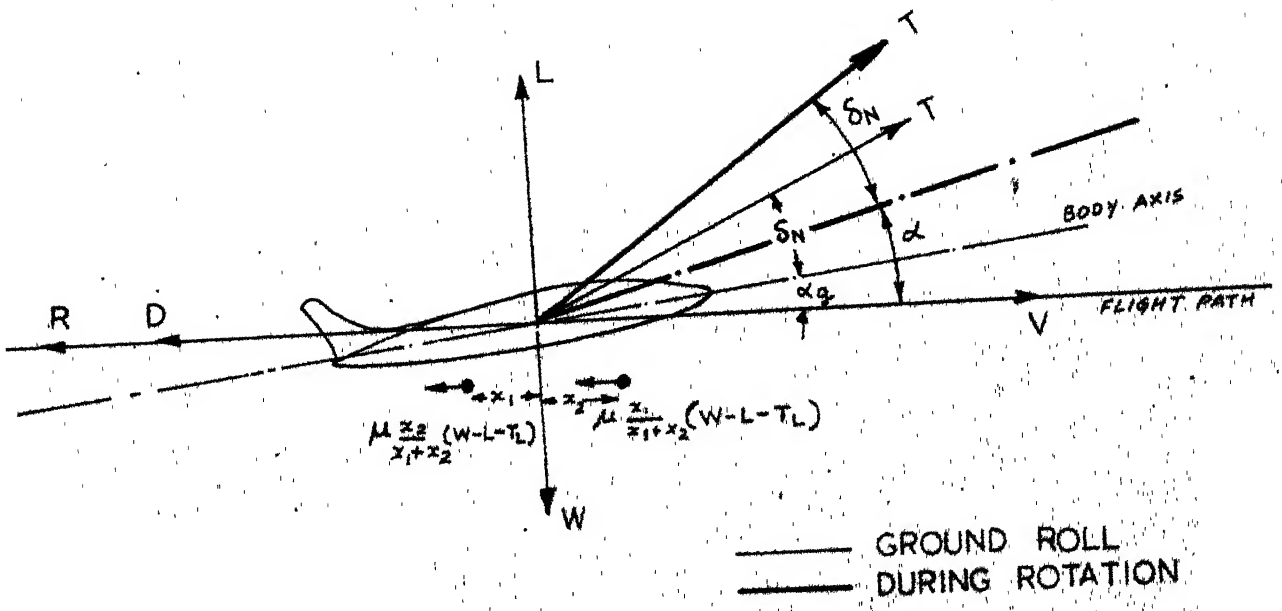
T
L
δ_N
T
δ_N
α
BODY AXIS
α_g
R
D
V
FLIGHT PATH
x_1
x_2
$\mu \frac{x_2}{x_1+x_2}(W-L-T_L)$
$\mu \frac{x_1}{x_1+x_2}(W-L-T_L)$
W
GROUND ROLL
DURING ROTATION

FIG. 2

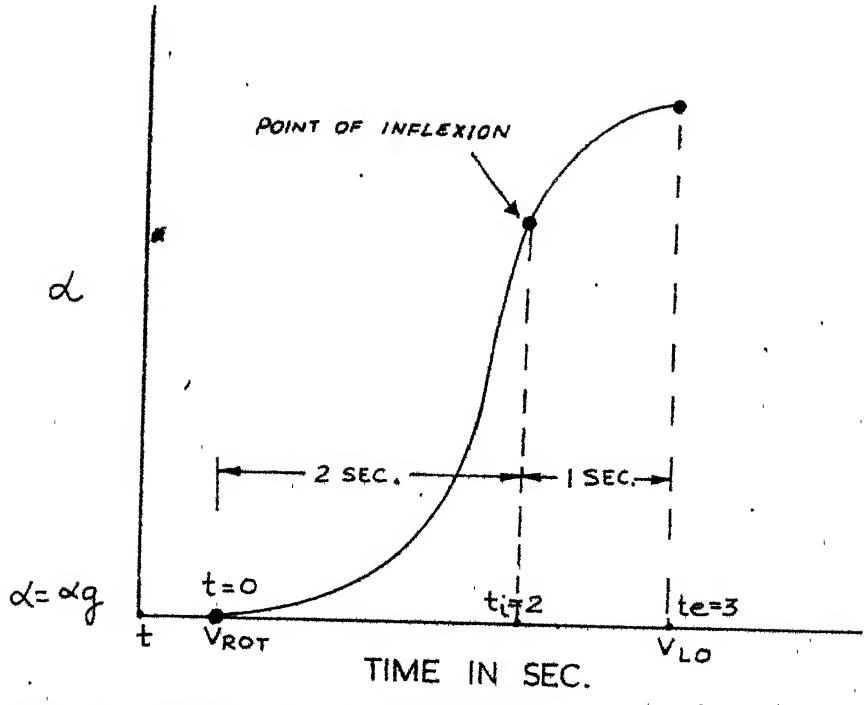

FIG. 3 – RATE AND PATTERN OF ROTATION

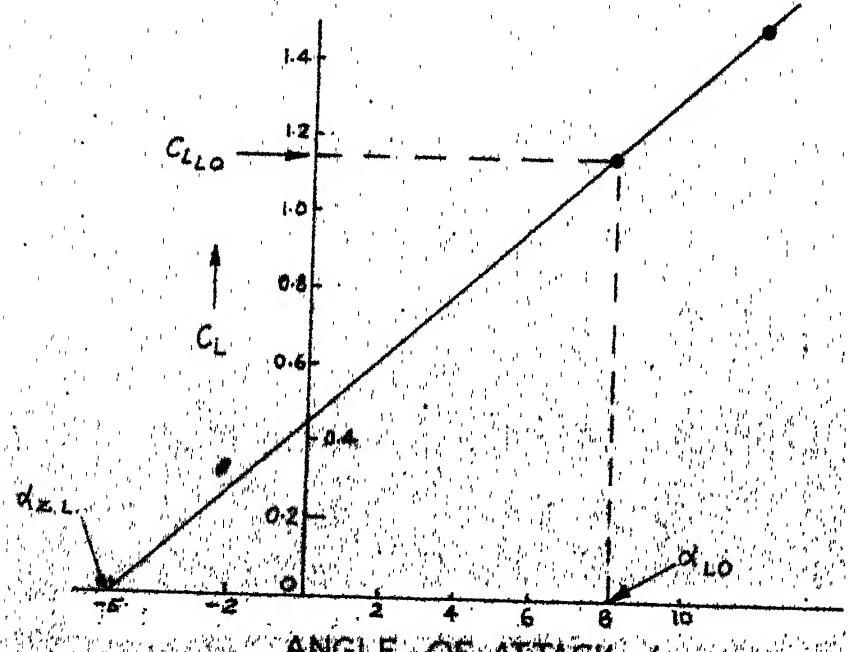

FIG. 4 – $C_L - \alpha$ CURVE

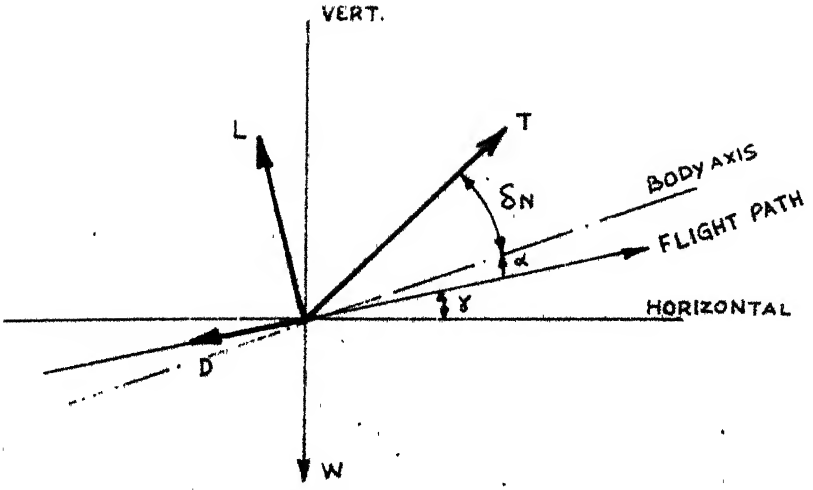

FORCES

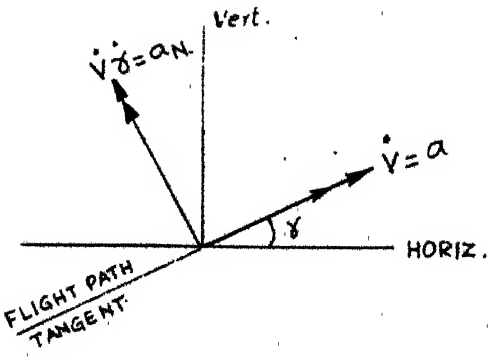

ACCELERATIONS

FIG. 5

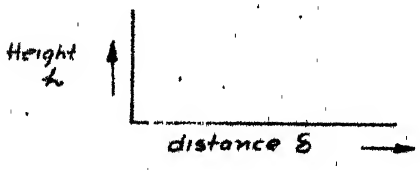

PISPLACEMENTS

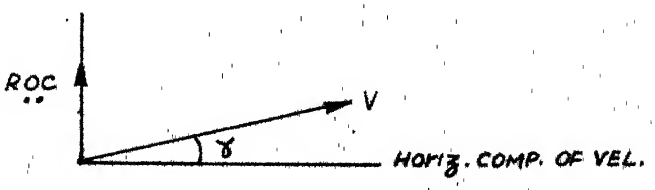

VELOCITIES

A TYPICAL FLIGHT PROFILE

A-B, B-50] NOZZLE DEFLECTED TO OPTIMUM ANGLE FOR T.O

50-E NOZZLE DEFLECTION GRADUALLY DECREASED TOWARDS HORIZONTAL

E-F - NOZZLE HORIZONTAL

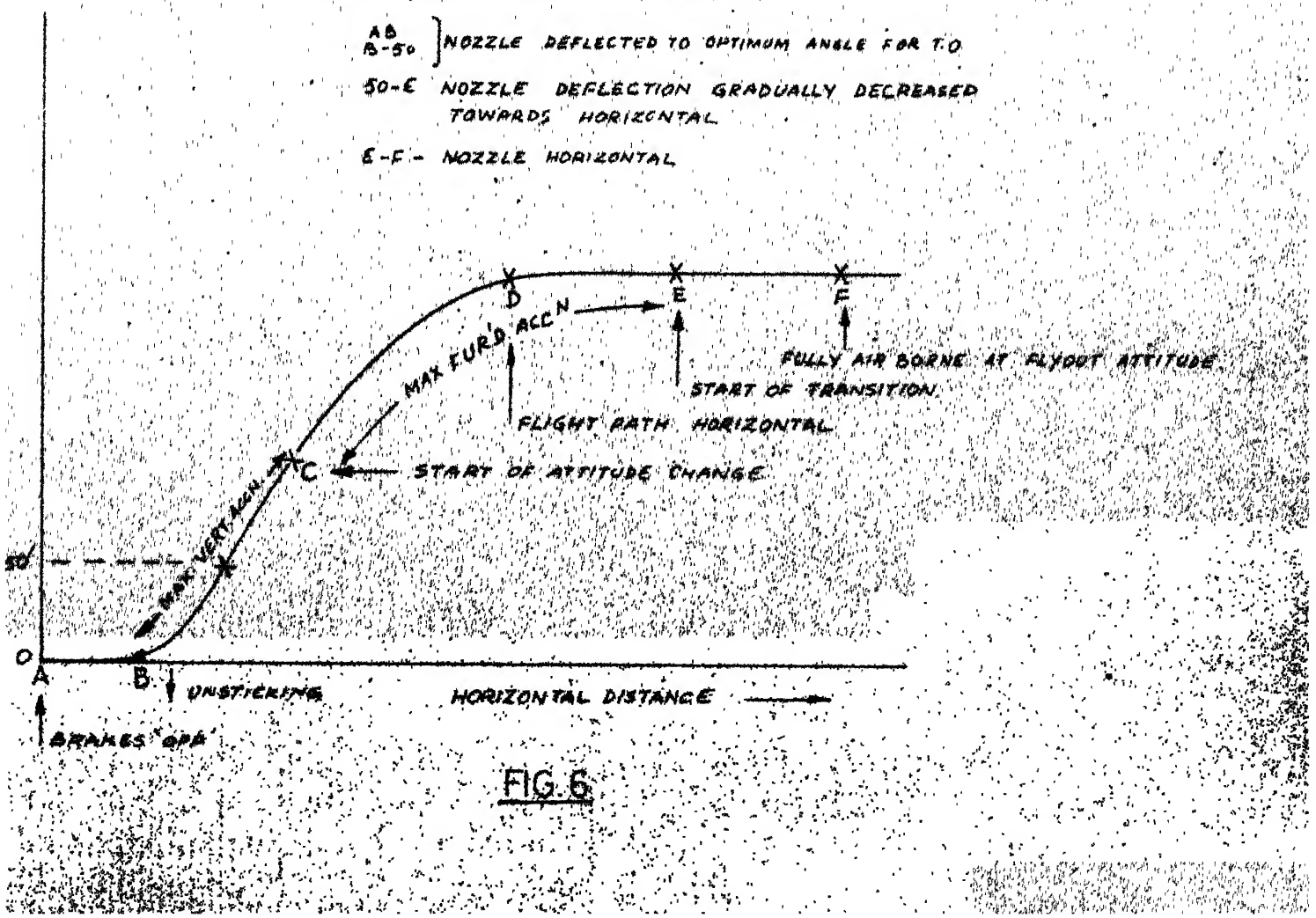

FIG. 6

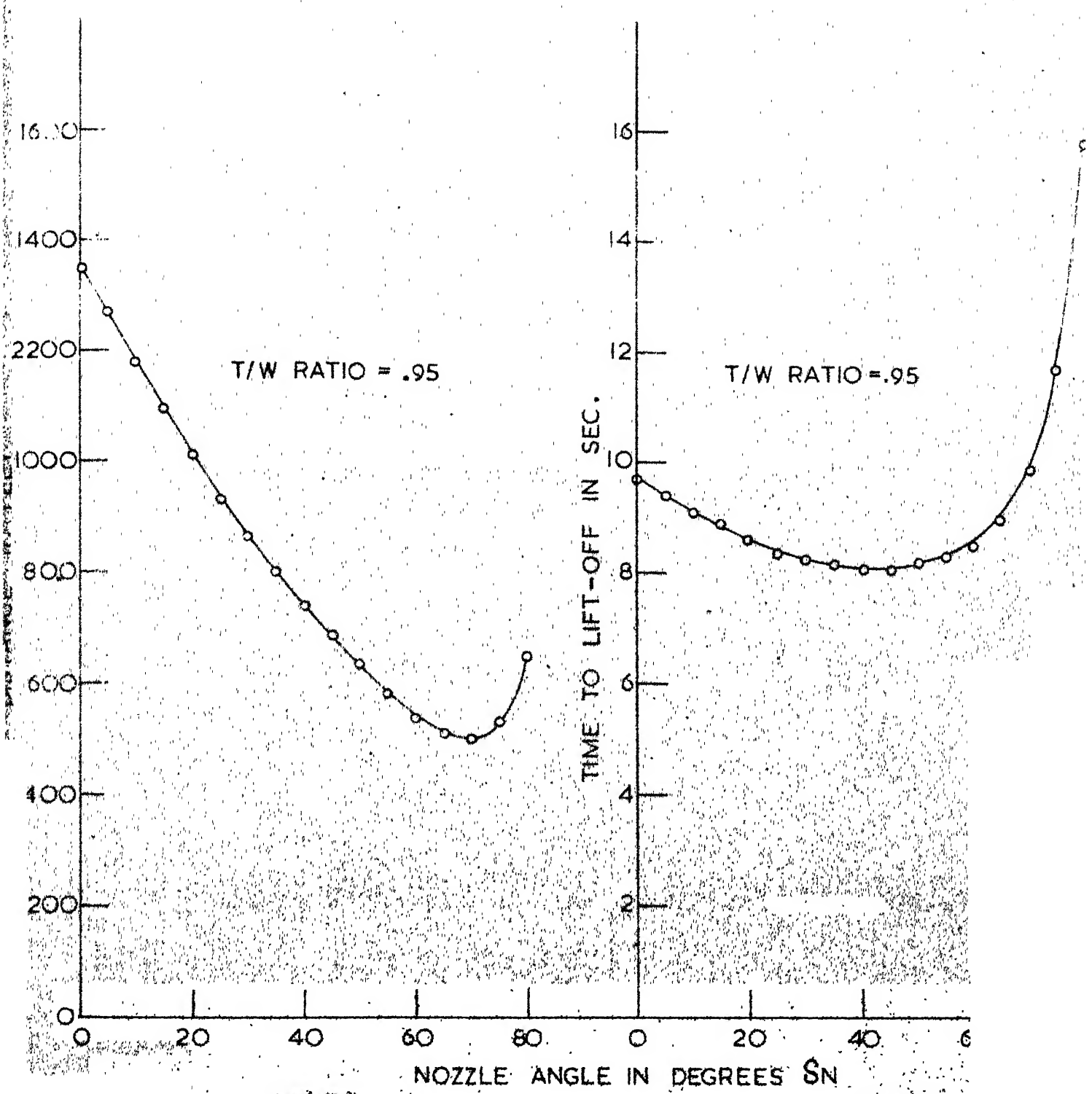

FIG. 7

FIG. 8

LIFT-OFF DISTANCE V/S NOZZLE ANGLE

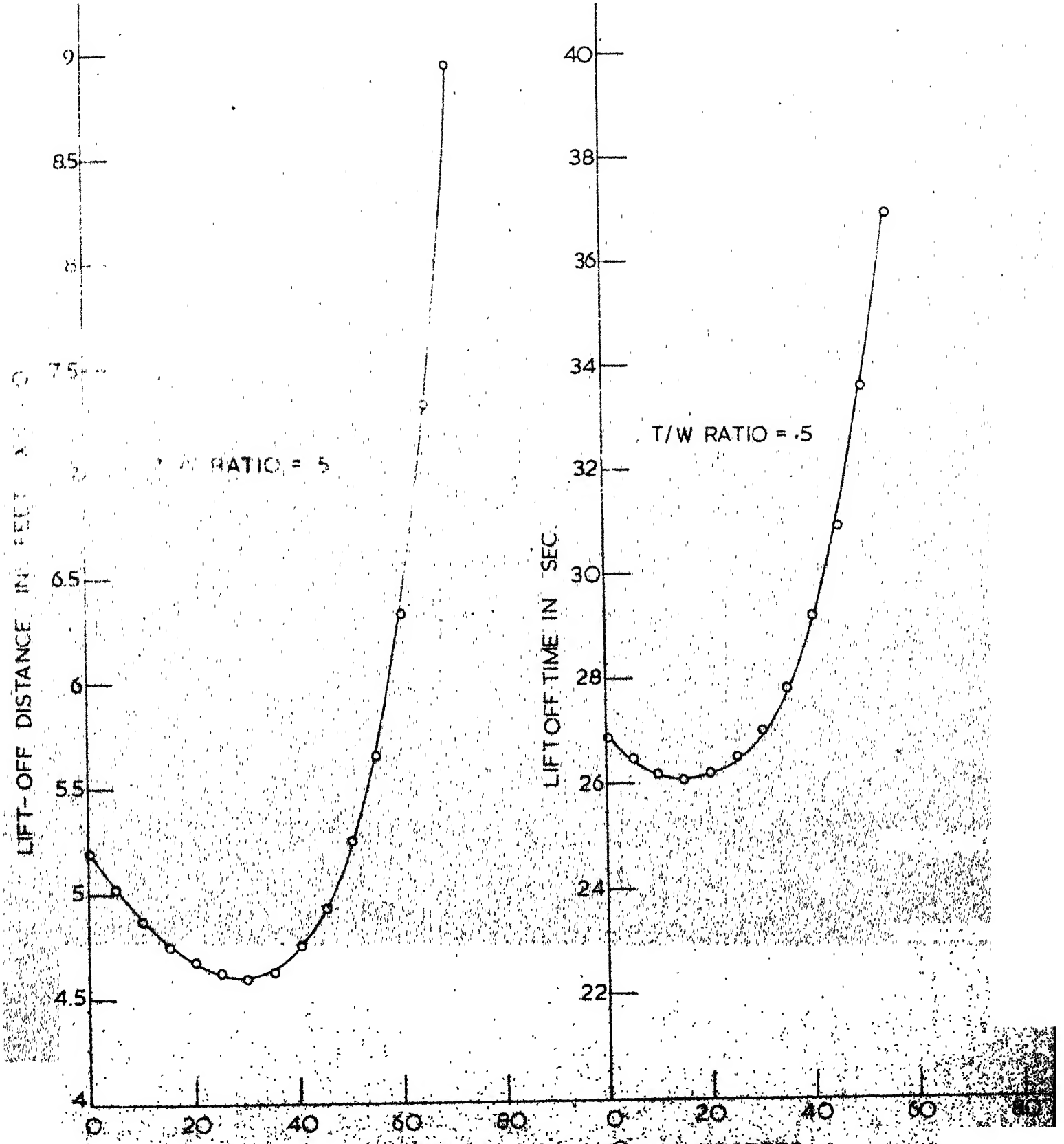

FIG. 9 LIFT-OFF DISTANCE V/S NOZZLE ANGLE FIG. 10

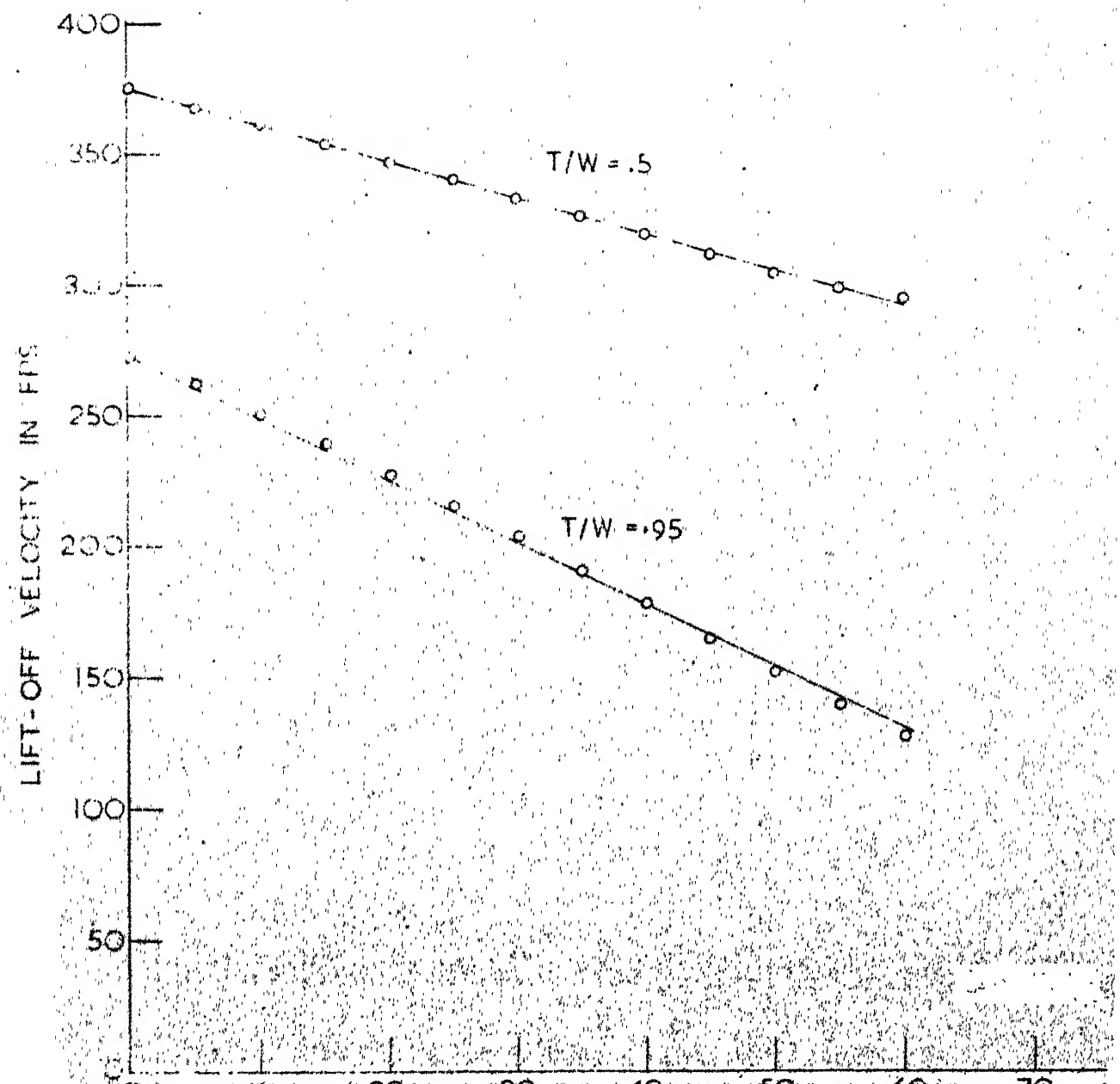

FIG II - LIFT-OFF VELOCITY V/S NOZZLE ANGLE

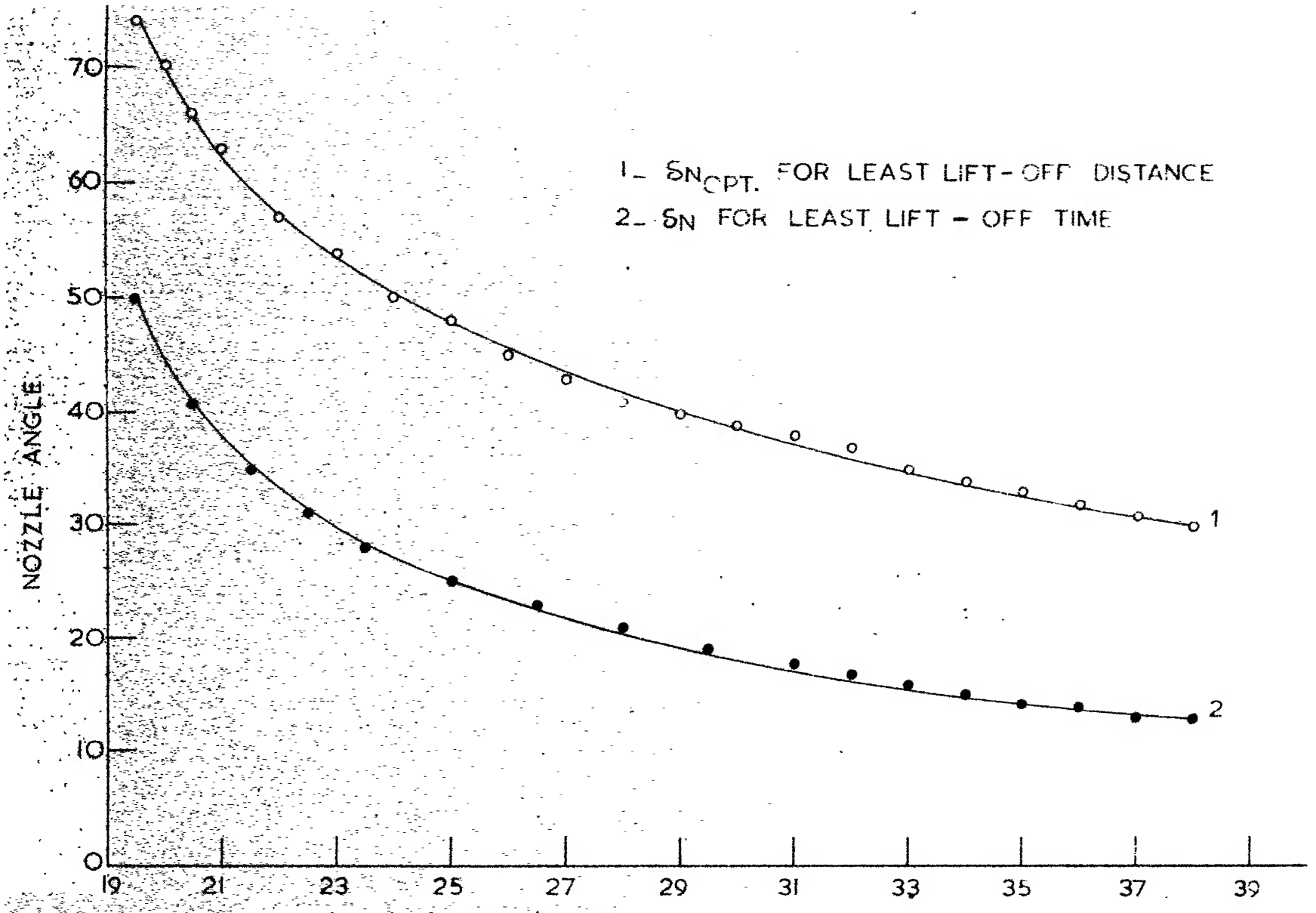

FIG 12_OPTIMUM NOZZLE ANGLES 1_FOR LEAST LIFT - OFF DISTANCE
2_LEAST LIFT-OFF TIME

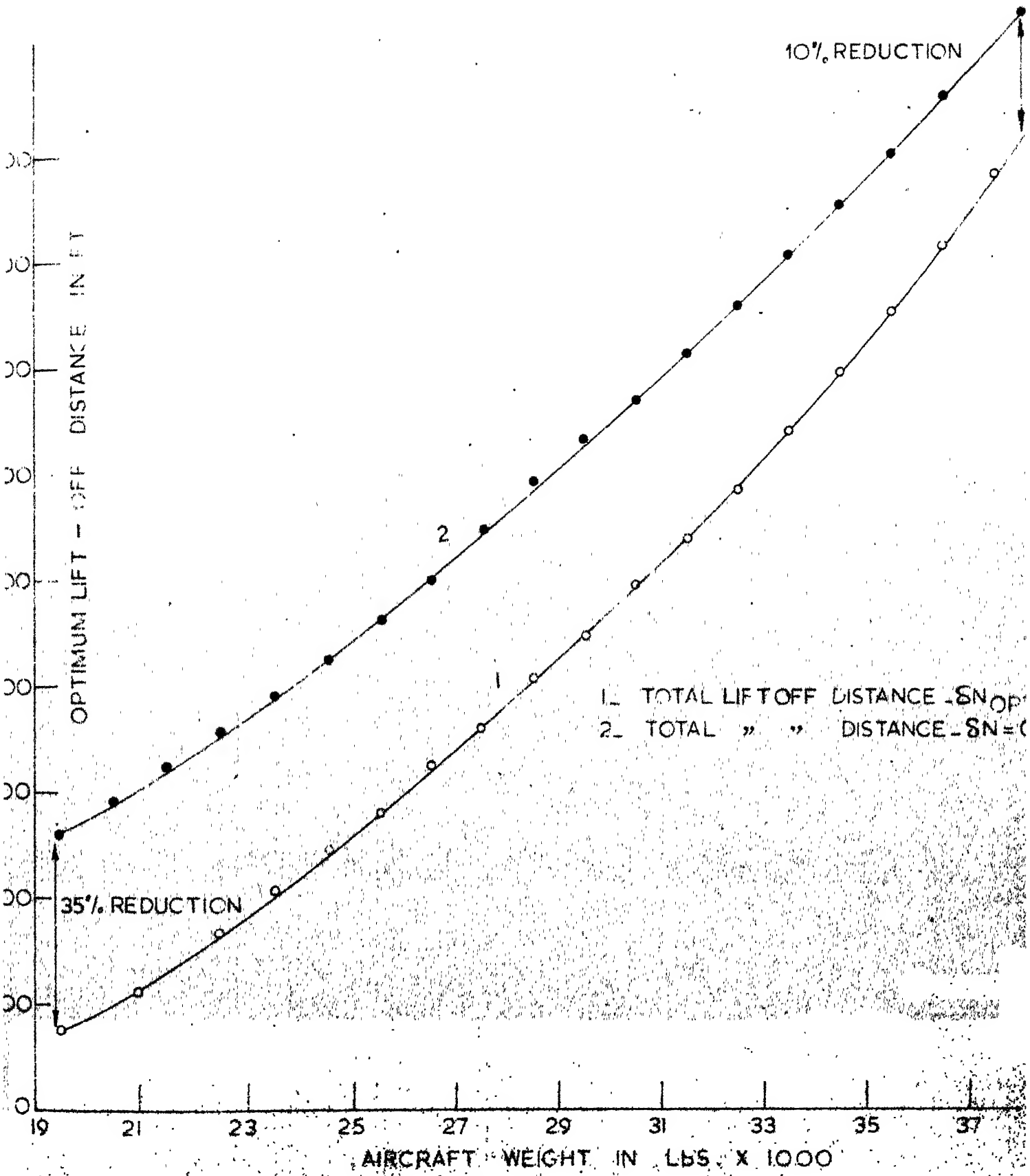

FIG 13_ LIFT-OFF GROUND DISTANCE 1_OPTIMUM 2_CONVENTIONAL

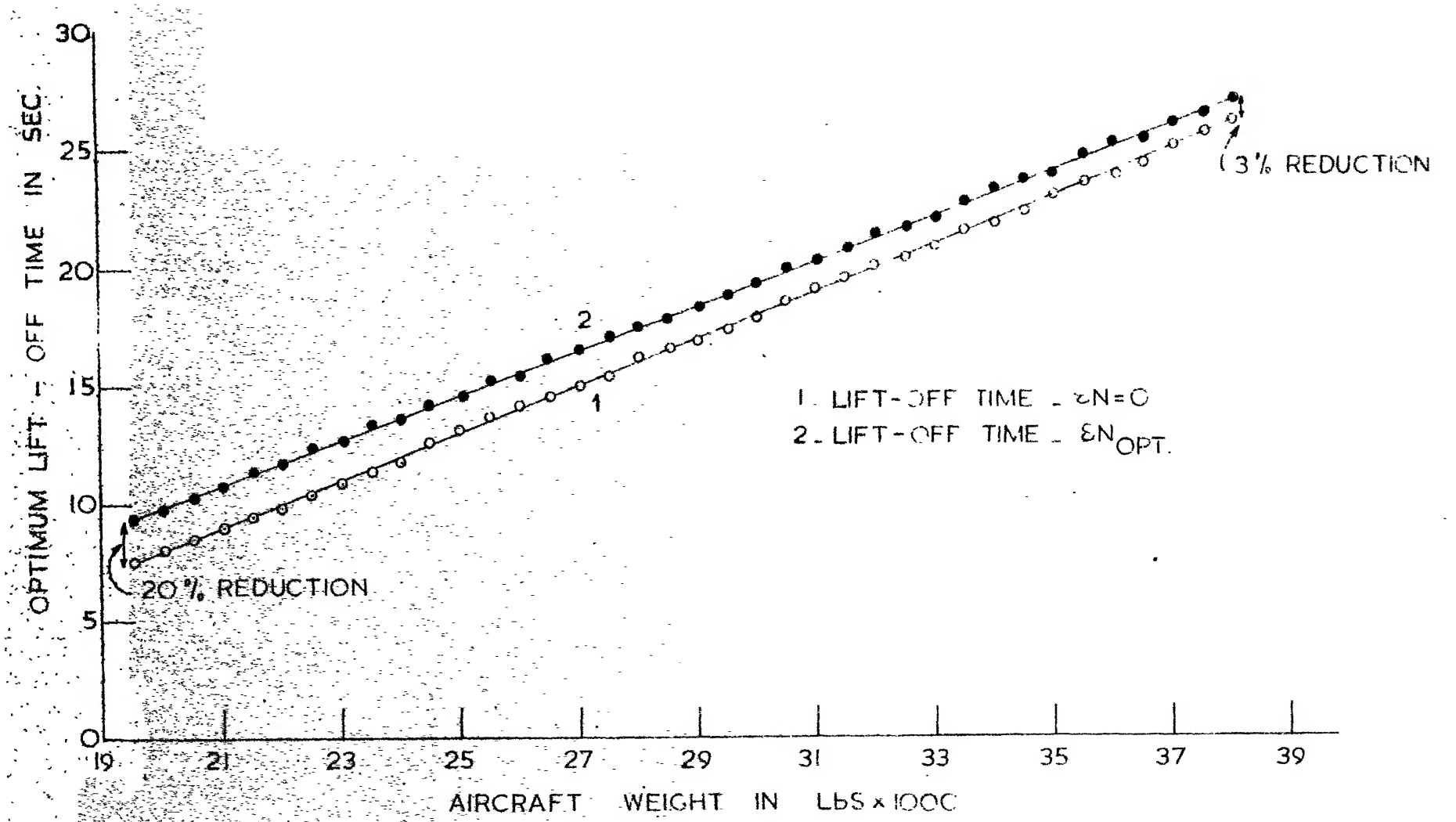

FIG.14 - TIME TO LIFT-OFF 1 - OPTIMUM
2 - CONVENTIONAL

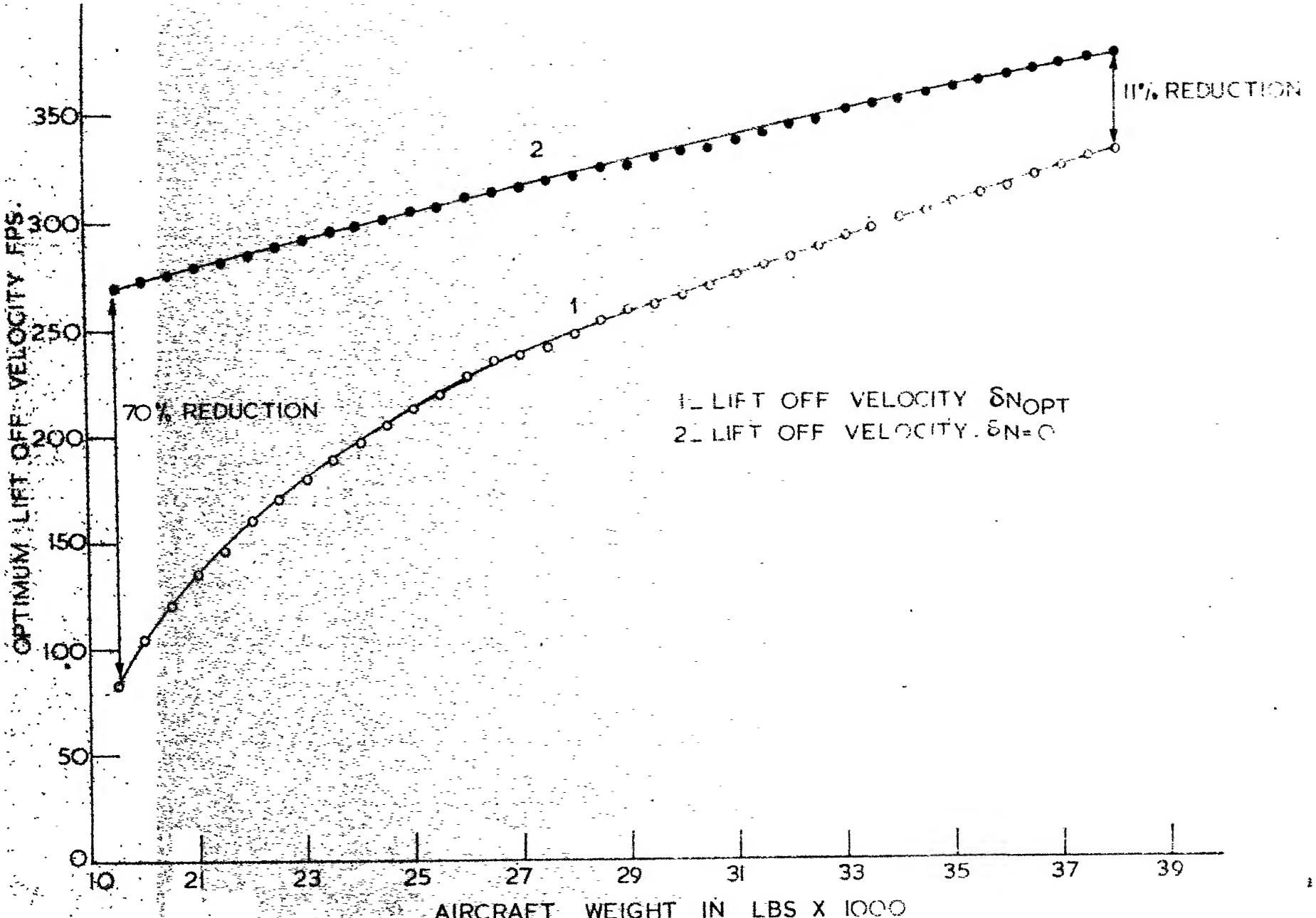

FIG. 15_ LIFT OFF VELOCITY 1_ OPTIMUM 2_ CONVENTIONAL

$C_{L_{Max}}$ VARIATION WITH MACH NO.

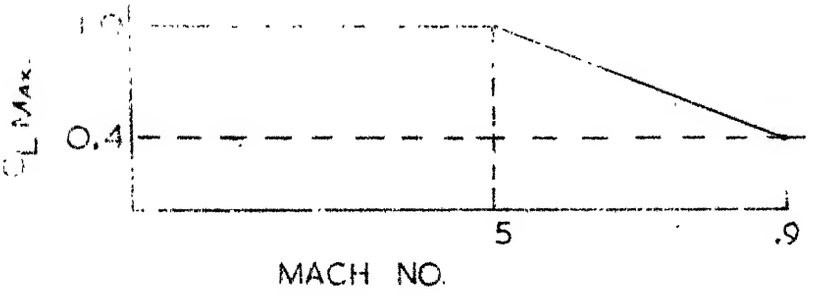

$C_{L\,MAX} = f(M)$

$C_{L\,MAX} = 1.0$ FOR $M < 0.5$

$C_{L\,MAX} = 1.75 - 1.5M$ FOR $M > 0.5$

FIG. 16

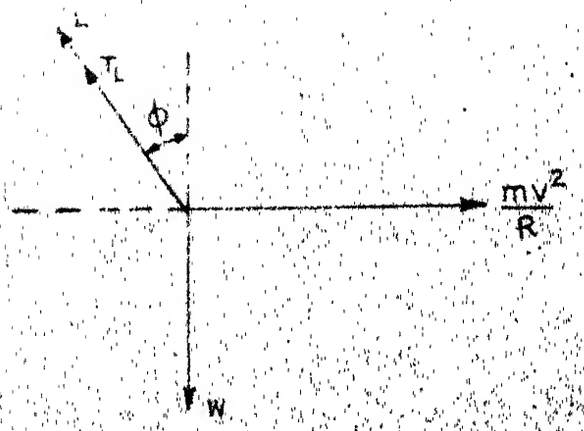

FIG. 17

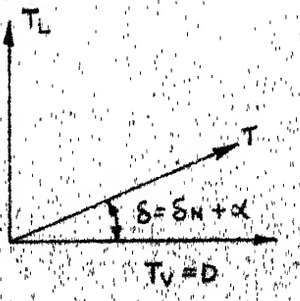

FIG. 18

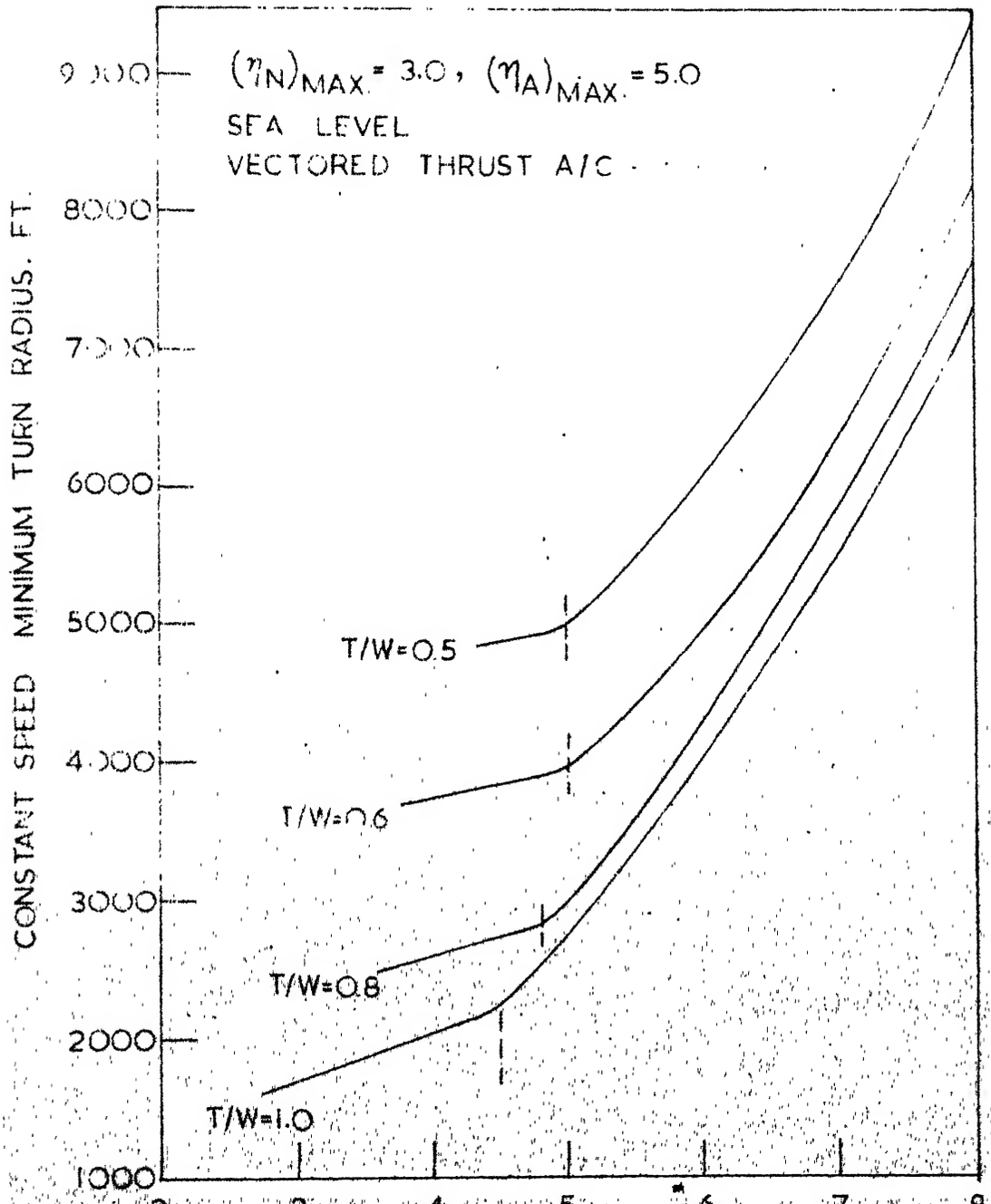
$(\eta_N)_{MAX.} = 3.0$, $(\eta_A)_{MAX.} = 5.0$
SEA LEVEL
VECTORED THRUST A/C
CONSTANT SPEED MINIMUM TURN RADIUS, FT.
9000
8000
7000
6000
5000
4000
3000
2000
1000
T/W=0.5
T/W=0.6
T/W=0.8
T/W=1.0
.2
.3
.4
.5
.6
.7
.8
MACH NO.

FIG. 19

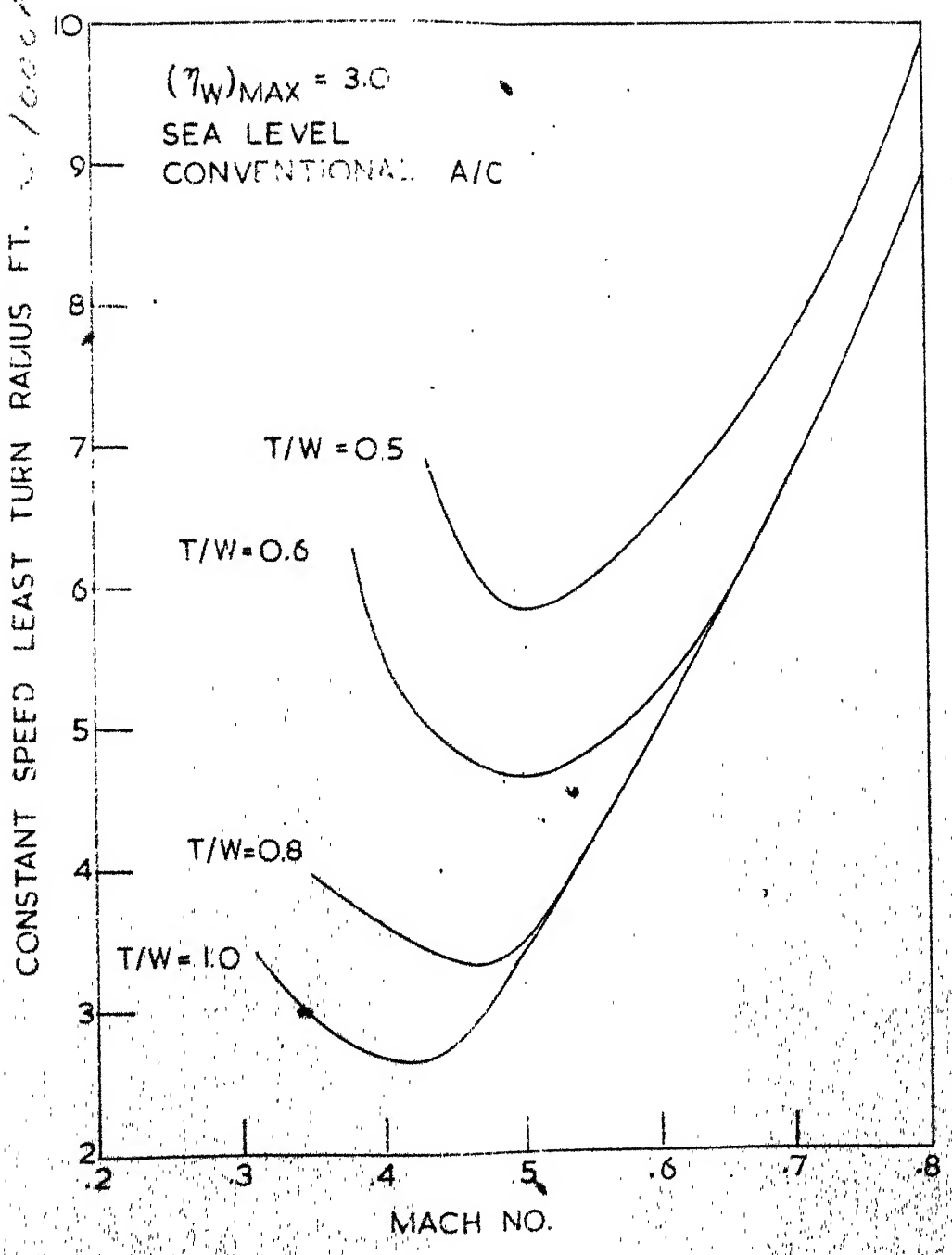
$(\eta_W)_{MAX}$ = 3.0
SEA LEVEL
CONVENTIONAL A/C
T/W = 0.5
T/W = 0.6
T/W = 0.8
T/W = 1.0
CONSTANT SPEED LEAST TURN RADIUS FT.
MACH NO.
10
9
8
7
6
5
4
3
2
.2
.3
.4
.5
.6
.7
.8

FIG. 20

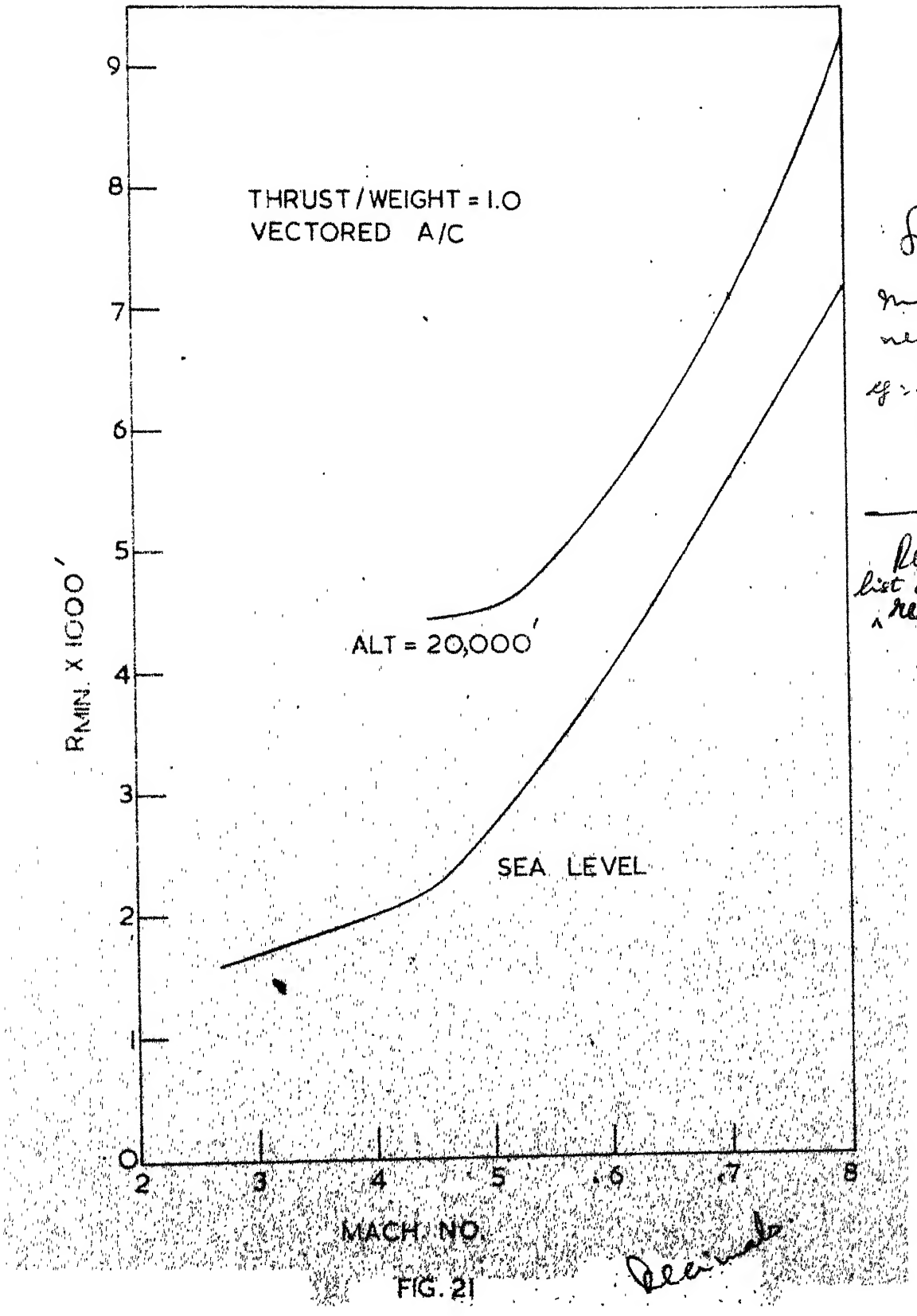

FIG. 21

fig 1-15; more info necessary: $\frac{T}{W}$ = ... ALT = ... W = ...

Reference in text ... list of references

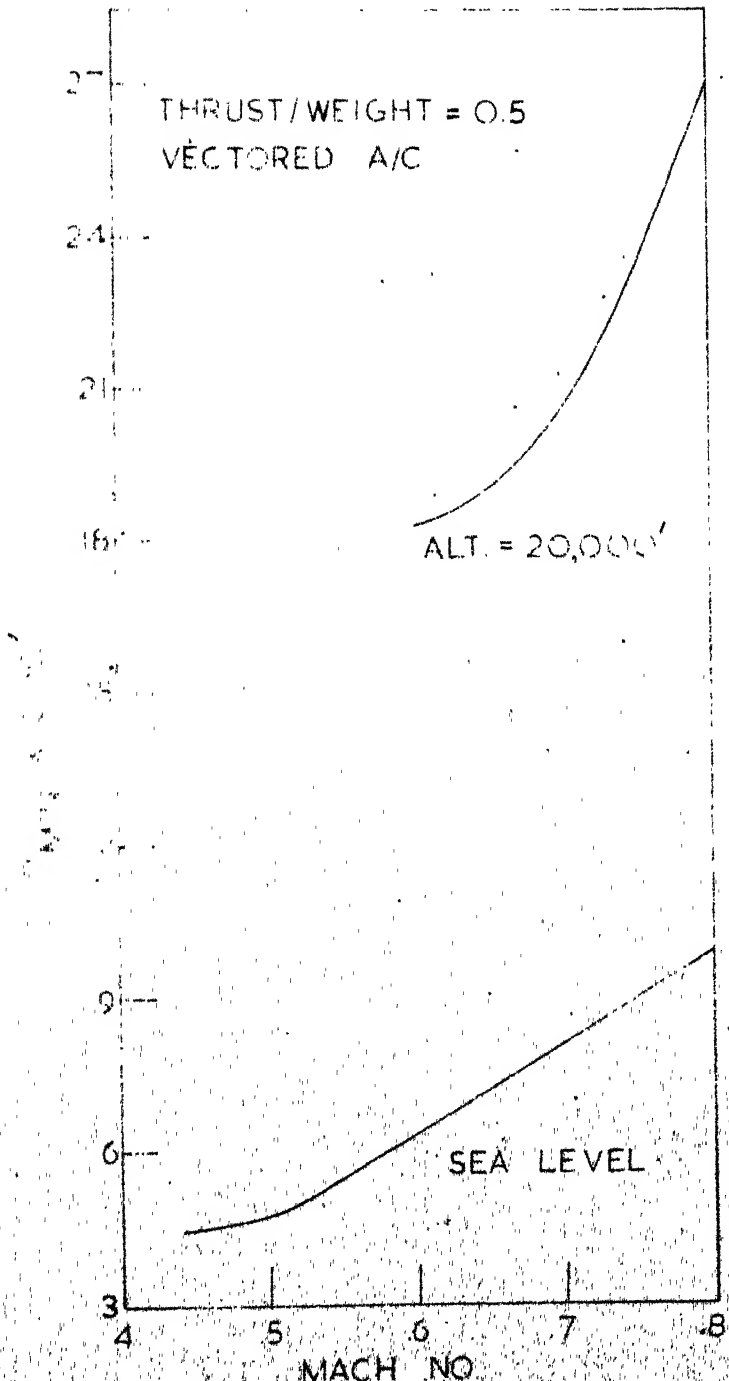

FIG. 22

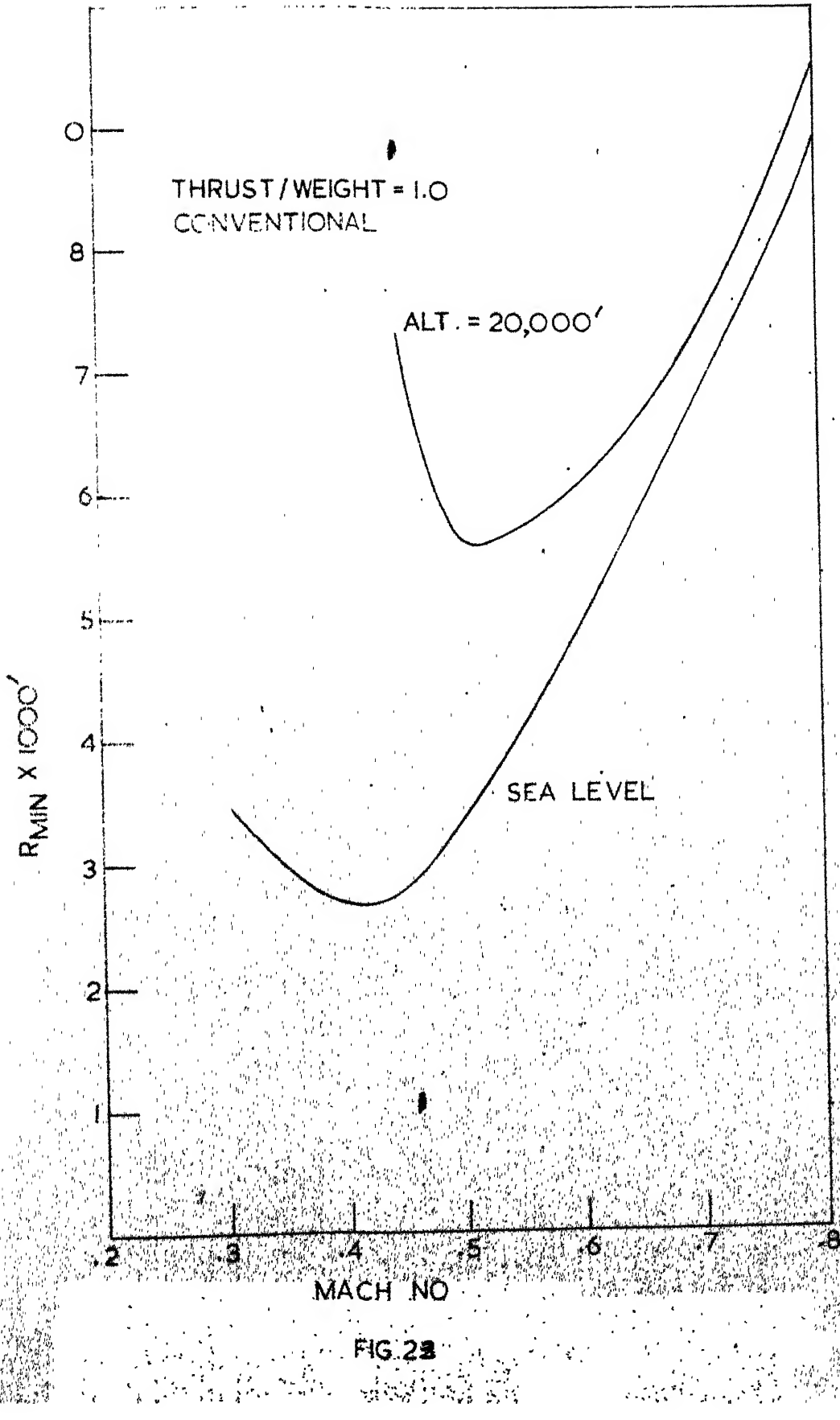
THRUST / WEIGHT = 1.0
CONVENTIONAL
ALT. = 20,000'
SEA LEVEL
R_{MIN} X 1000'
0
8
7
6
5
4
3
2
1
.2
.3
.4
.5
.6
.7
.8
MACH NO

FIG 23

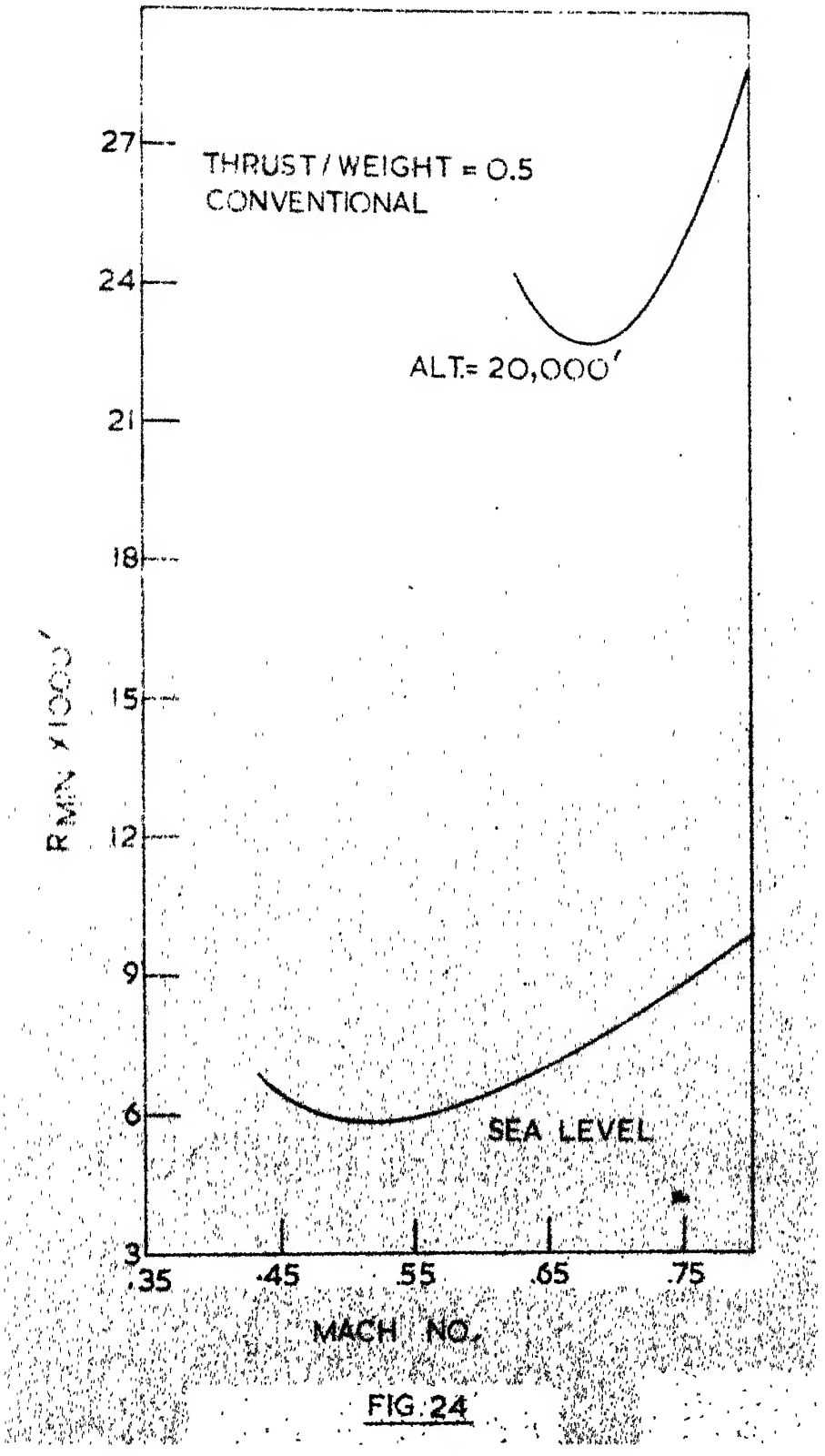
THRUST / WEIGHT = 0.5
CONVENTIONAL
ALT.= 20,000'
SEA LEVEL
R MIN. X 1000'
27
24
21
18
15
12
9
6
3
.35
.45
.55
.65
.75
MACH NO.

FIG. 24

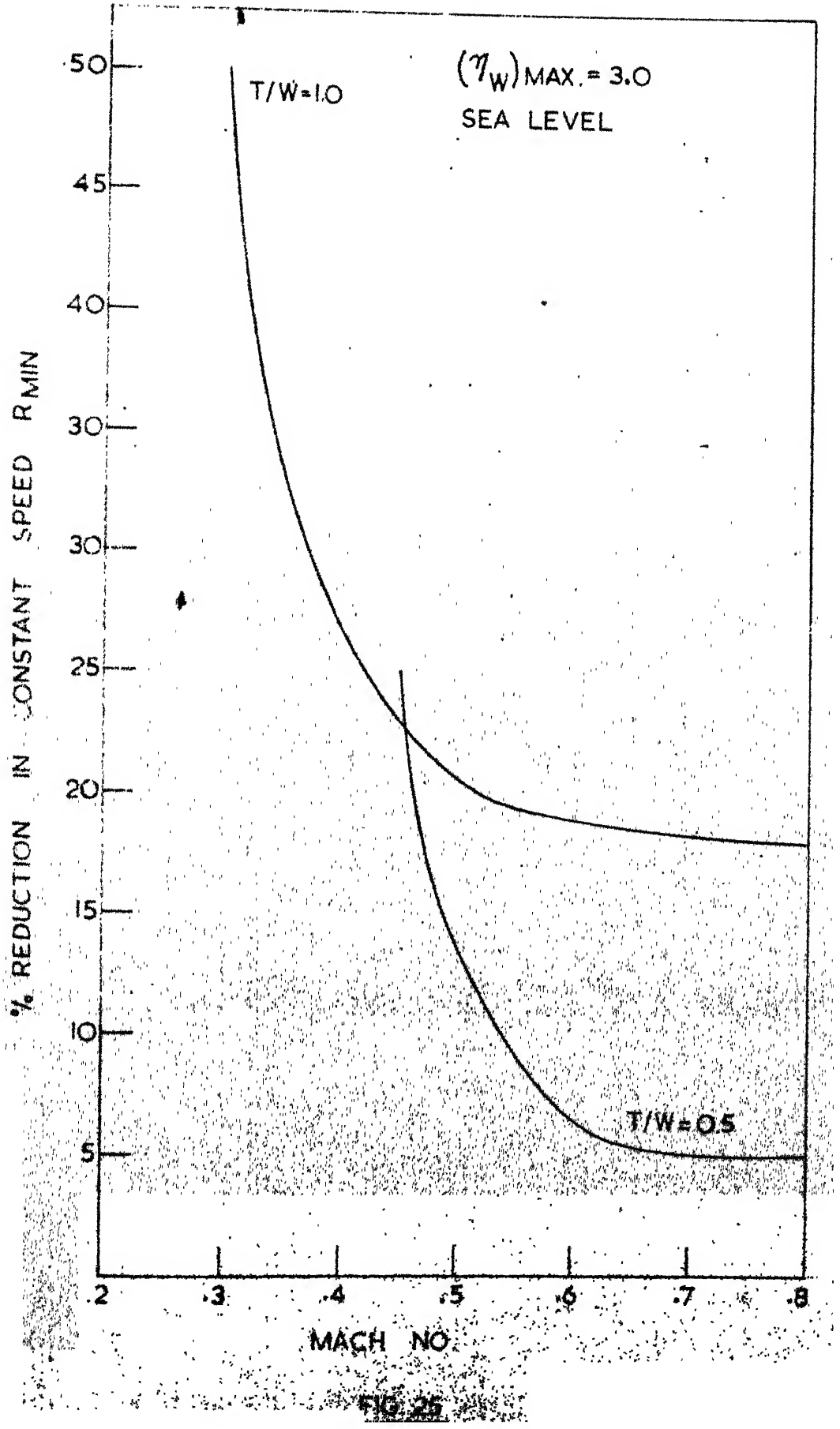
(η_W) MAX. = 3.0
SEA LEVEL
T/W=1.0
T/W=0.5
% REDUCTION IN CONSTANT SPEED R_{MIN}
50
45
40
30
30
25
20
15
10
5
.2
.3
.4
.5
.6
.7
.8
MACH NO.

FIG. 25

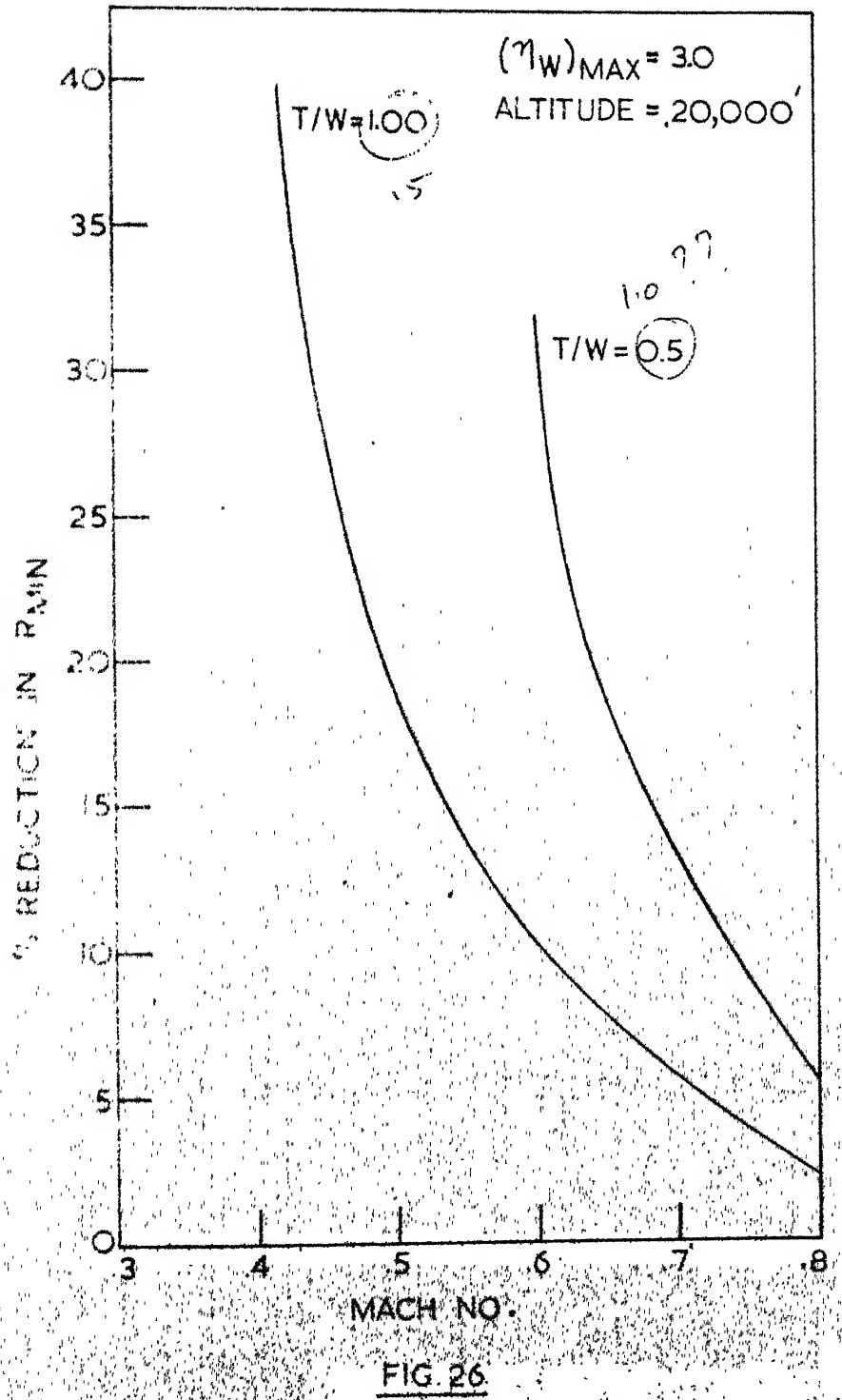
$(\eta_W)_{MAX}$ = 3.0
ALTITUDE = 20,000'
T/W = 1.00
T/W = 0.5
% REDUCTION IN R_{MIN}
0
5
10
15
20
25
30
35
40
3
4
5
6
7
8
MACH NO.

FIG. 26

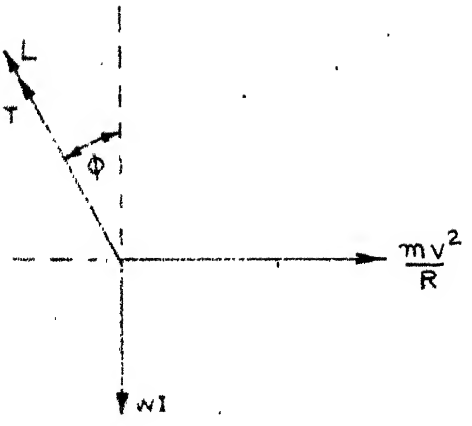

FIG 27_FORCE DIAGRAM OPTIMUM TURN

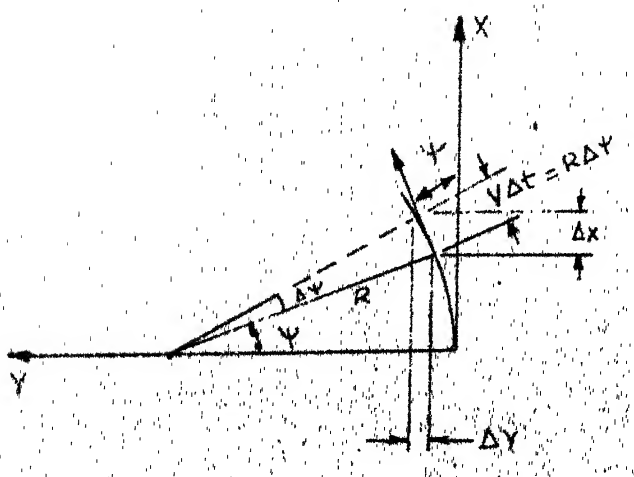

FIG. 28

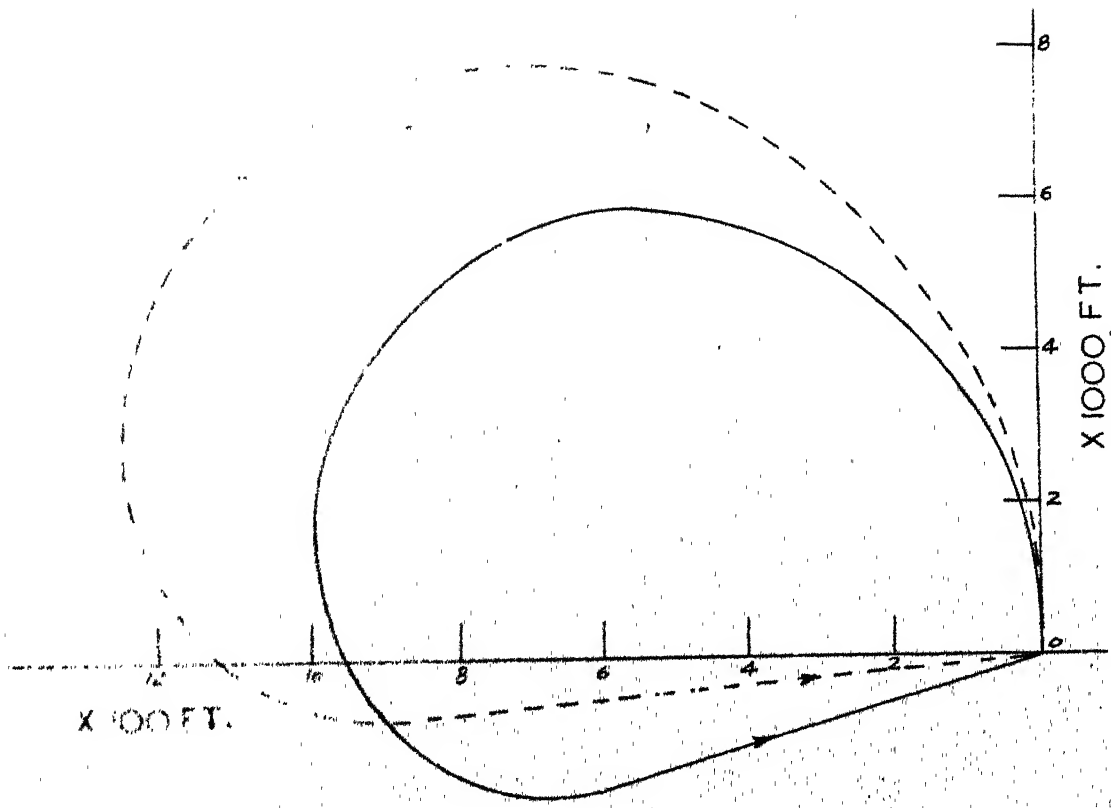

SEA LEVEL
THRUST / WEIGHT = 1.0
---- CONVENTIONAL
———— VECTORED

FIG. 29

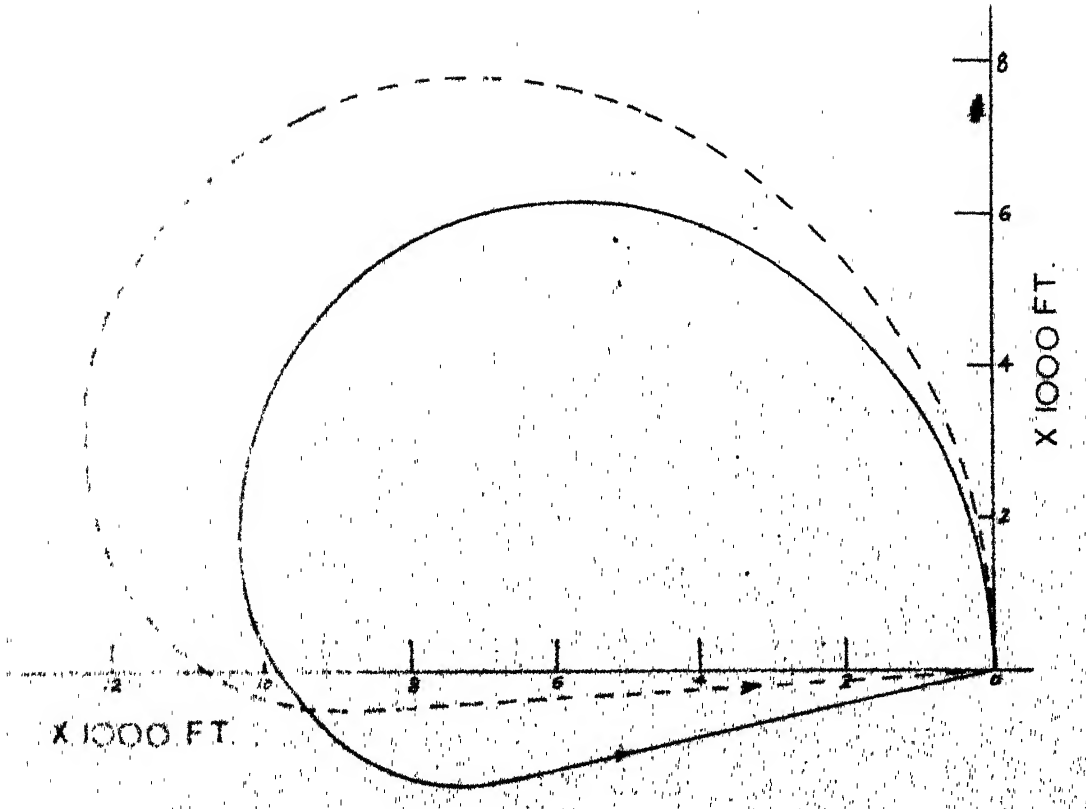

SEA-LEVEL
THRUST/WEIGHT = 0.8
----- CONVENTIONAL
—— VECTORED

FIG. 30

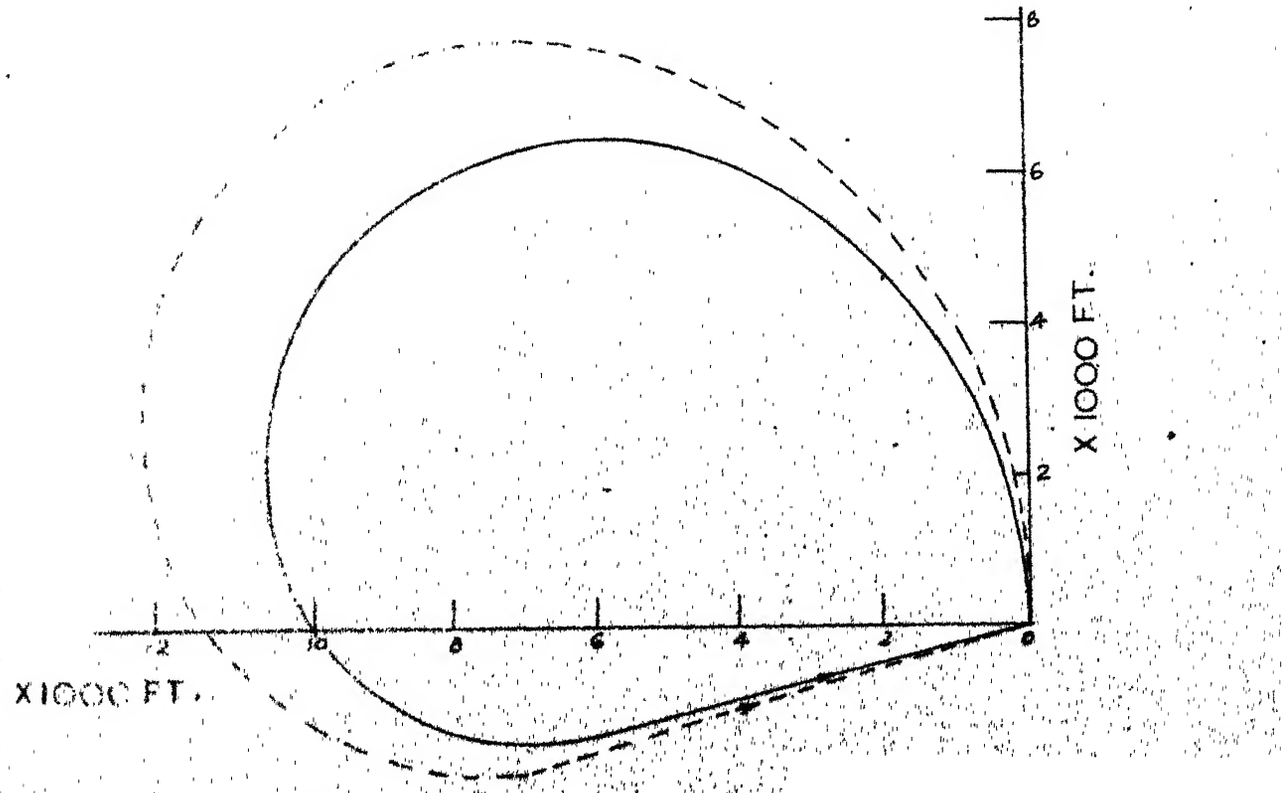

SEA-LEVEL
THRUST / WEIGHT = 0.6
– – – CONVENTIONAL
——— VECTORED

FIG. 31

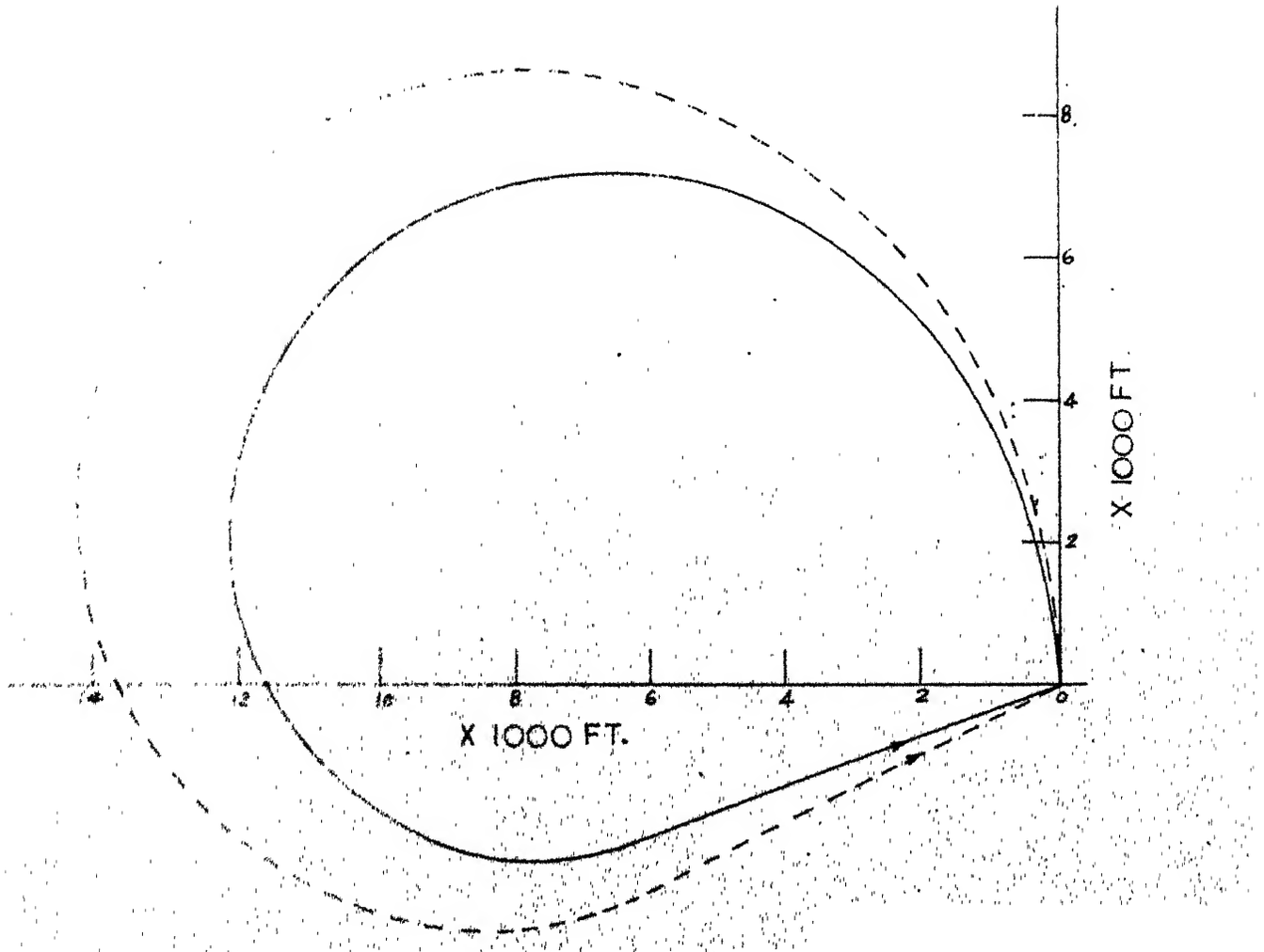

SEA - LEVEL
THRUST / WEIGHT = 0.5
- - - - - CONVENTIONAL
——— VECTORED

FIG 32

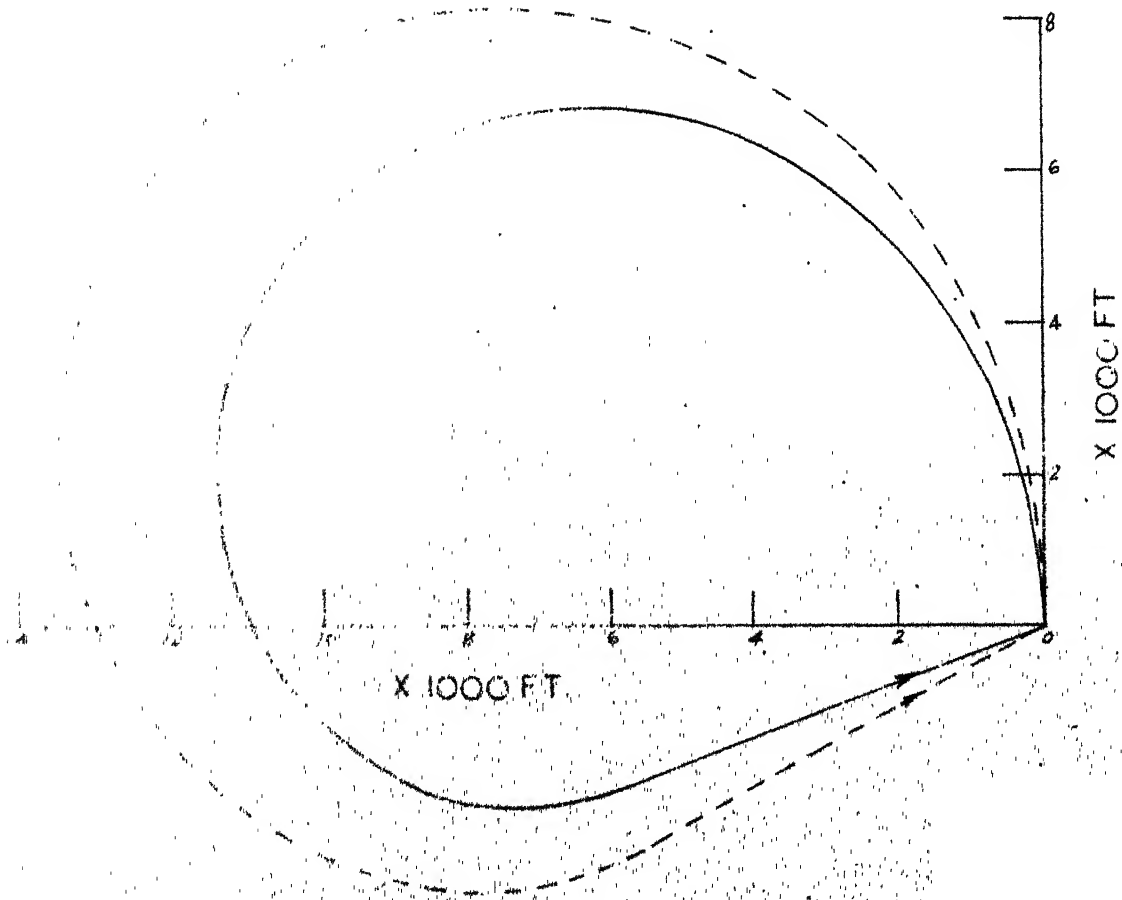

ALTITUDE = 20,000'
THRUST / WEIGHT = 1.0
——— CONVENTIONAL
– – – – VECTORED

FIG 33

ALTITUDE = 20,000'
THRUST/WEIGHT = 0.8
CONVENTIONAL
VECTORED
X 1000 FT.

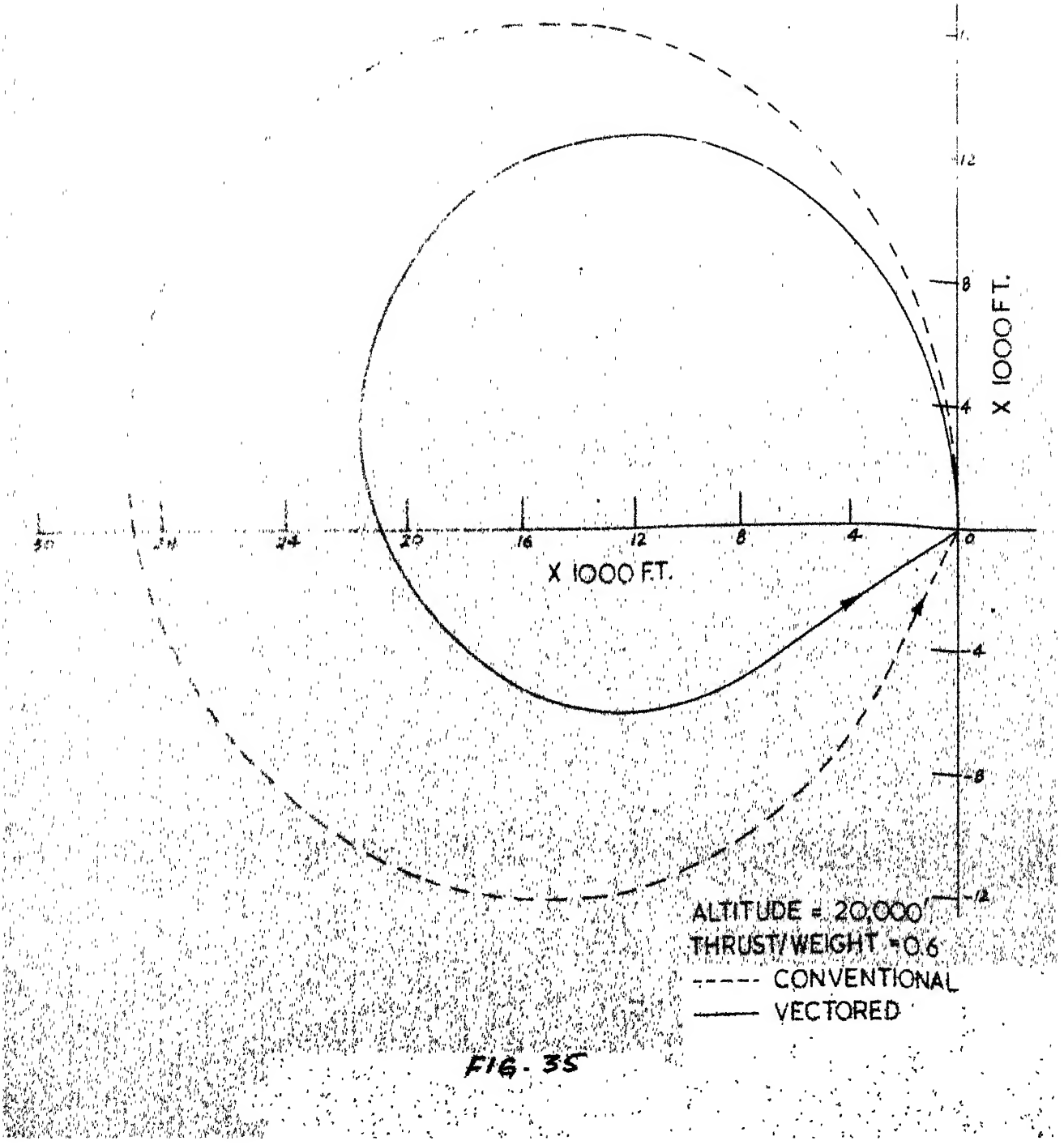
X 1000 FT.
X 1000 FT.
ALTITUDE = 20,000'
THRUST/WEIGHT = 0.6
CONVENTIONAL
VECTORED

FIG. 35

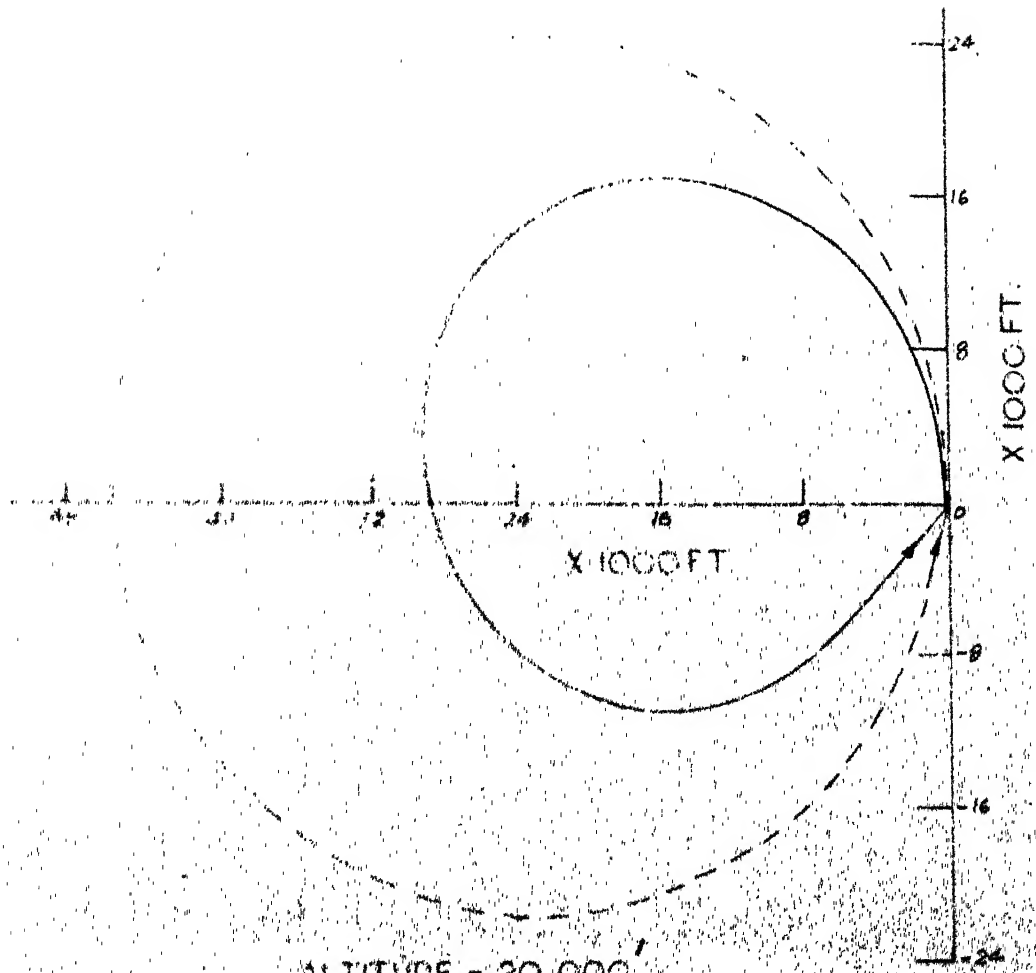

ALTITUDE = 20,000'
THRUST / WEIGHT = .05
- - - CONVENTIONAL
——— VECTORED

FIG 36

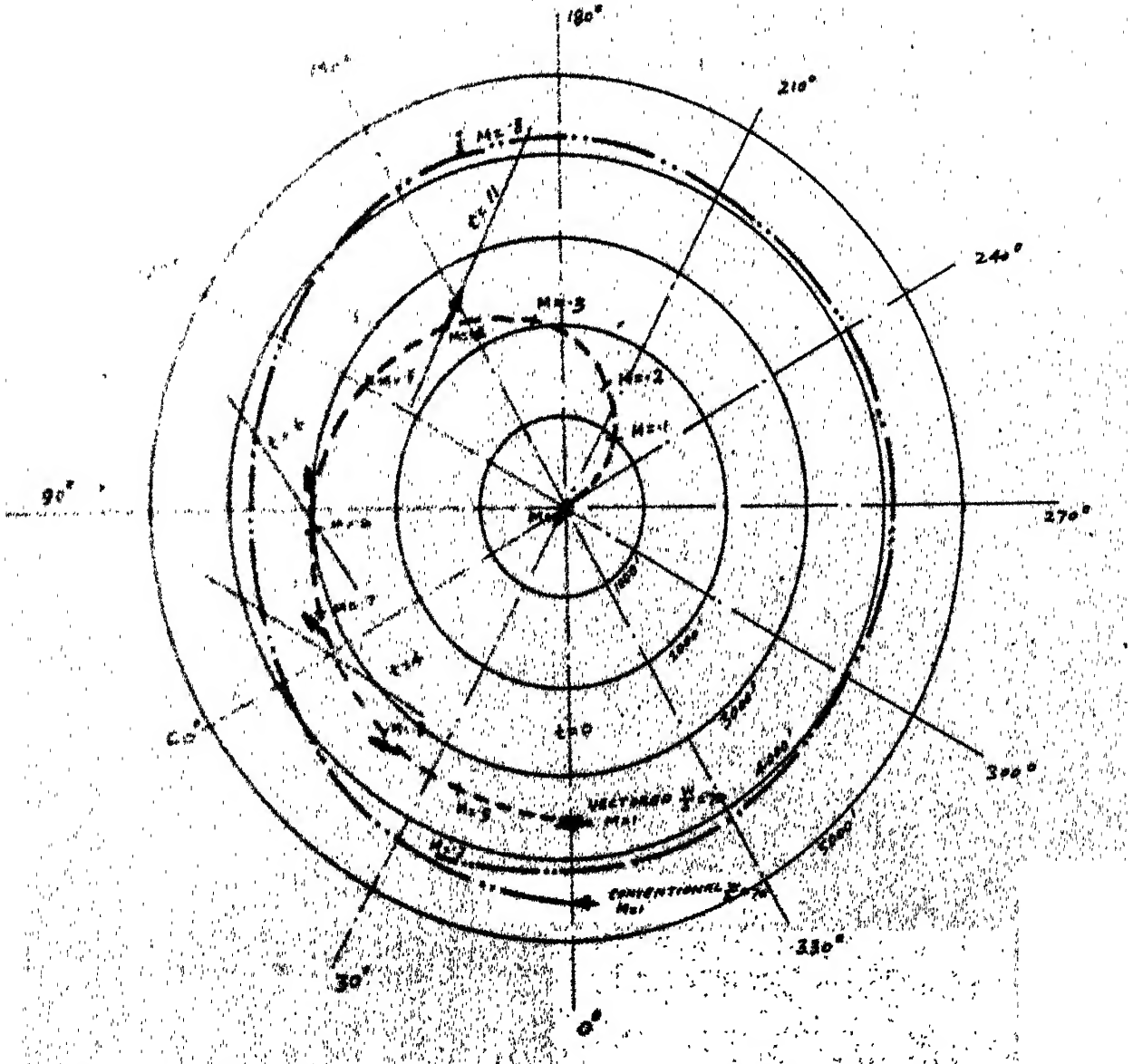

FIG. 37_ A TYPICAL ... ETHOD BY NACA'S DUAL ... MANUE...

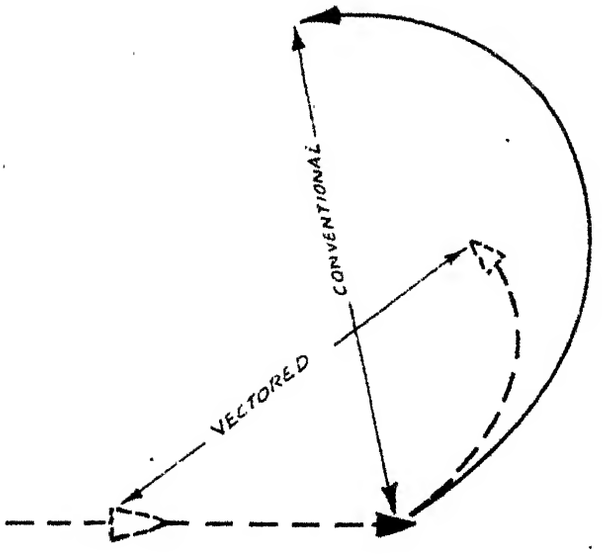

FIG. 38 - SHOWS RELATIVE TURNS CAPABILITY OF VECTORED THRUST (DOTTED) V/S CONVENTIONAL (FIRM). VECTORED THRUST A/C ATTACKS CONVENTIONAL AND TURNS INSIDE THE MINIMUM RADIUS OF CONVENTIONAL A/C.

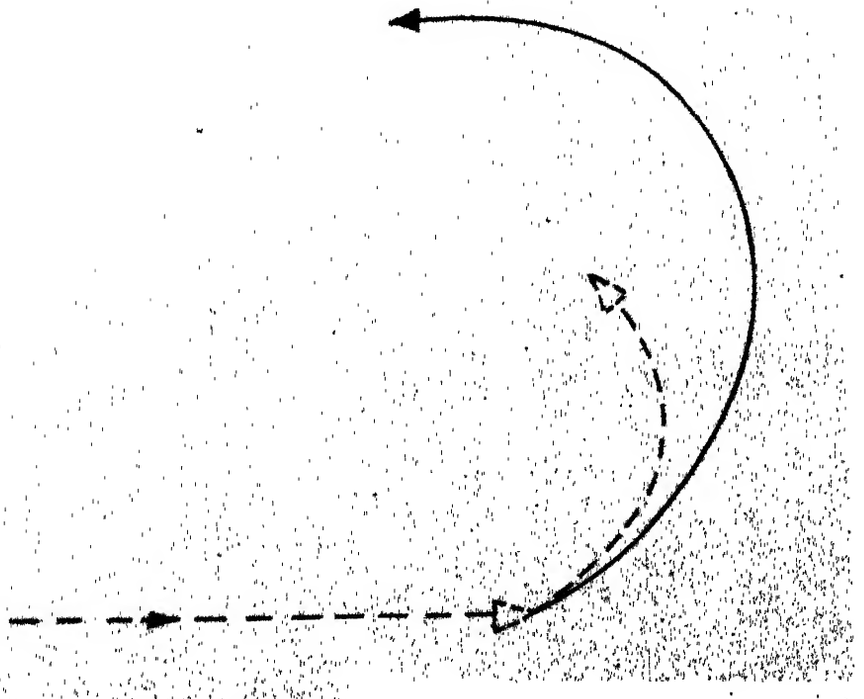

FIG. 39 - CONVENTIONAL ATTACKS VECTORED WHICH TURNS LEFT TO EVADE THE ATTACK. RAPID DECELERATION OF VECTORED CAUSES CONVENTIONAL TO TURN OUTSIDE AND OVER SHOOT. THIS TECHNIQUE HAS BEEN POPULARLY NAMED AS "SQUARE CORNER TURN."

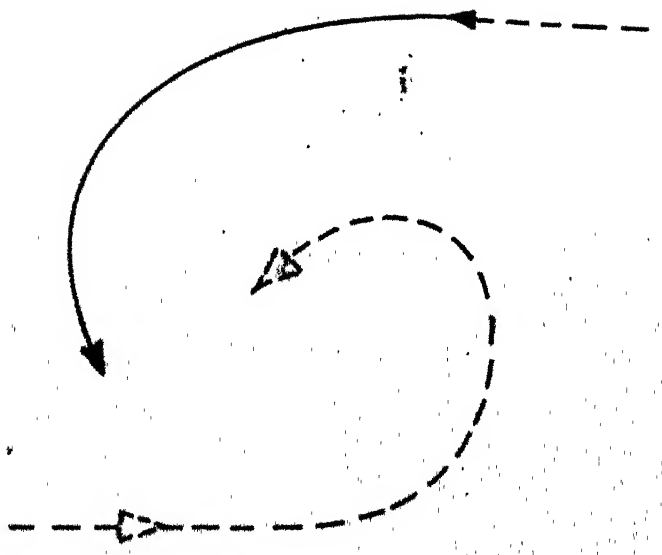

FIG. 40. AIRCRAFTS MEET "HEAD-ON" WITH CONVENTIONAL TURNING TO ATTACK BUT VECTORED THRUST TURNS A TIGHTER RADIUS.

FLOW CHART — LIFT OFF PERFORMANCE

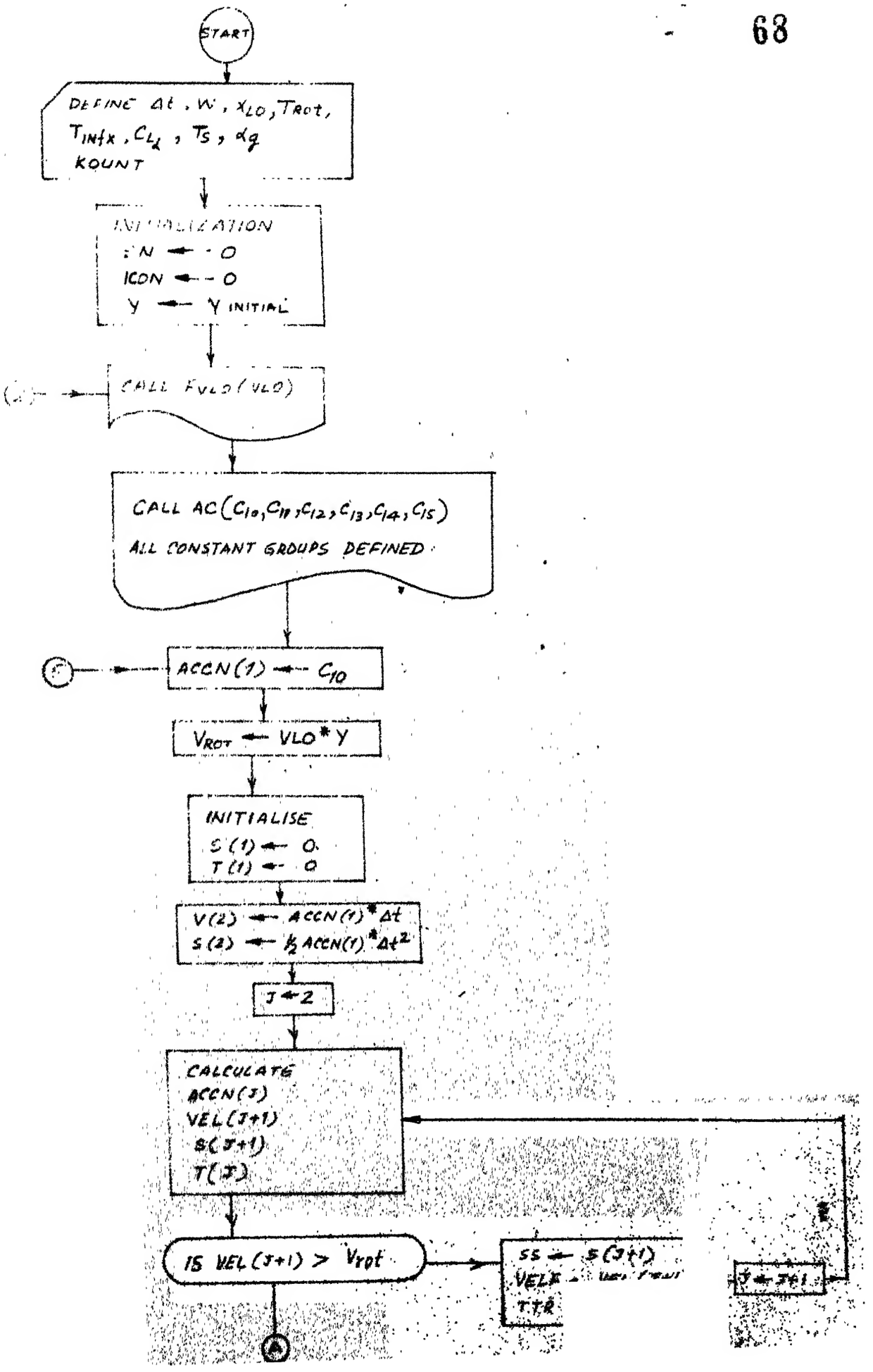

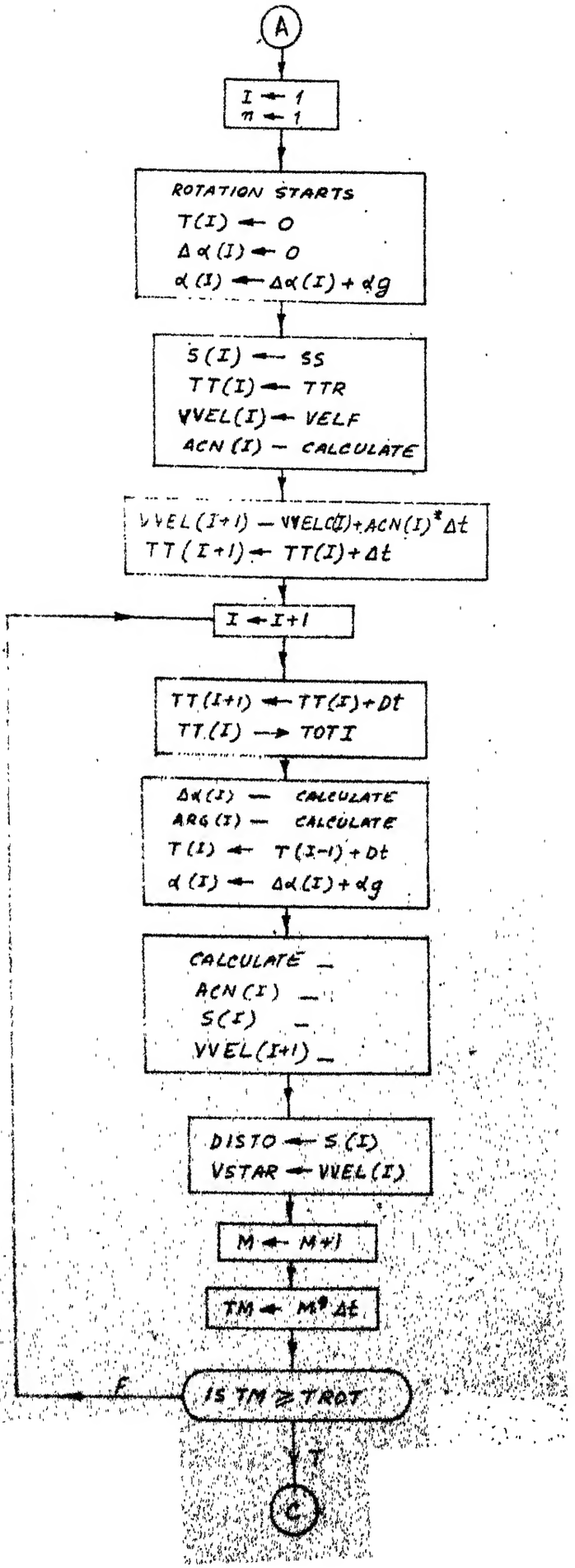
A
I ← 1
n ← 1
ROTATION STARTS
T(I) ← 0
Δα(I) ← 0
α(I) ← Δα(I) + αg
S(I) ← SS
TT(I) ← TTR
VVEL(I) ← VELF
ACN(I) — CALCULATE
VVEL(I+1) — VVEL(I) + ACN(I) * Δt
TT(I+1) ← TT(I) + Δt
I ← I+1
TT(I+1) ← TT(I) + Dt
TT(I) → TOTI
Δα(I) — CALCULATE
ARG(I) — CALCULATE
T(I) ← T(I-1) + Dt
α(I) ← Δα(I) + αg
CALCULATE —
ACN(I) —
S(I) —
VVEL(I+1) —
DISTO ← S(I)
VSTAR ← VVEL(I)
M ← M+1
TM ← M * Δt
IS TM ≥ TROT
F
T
C

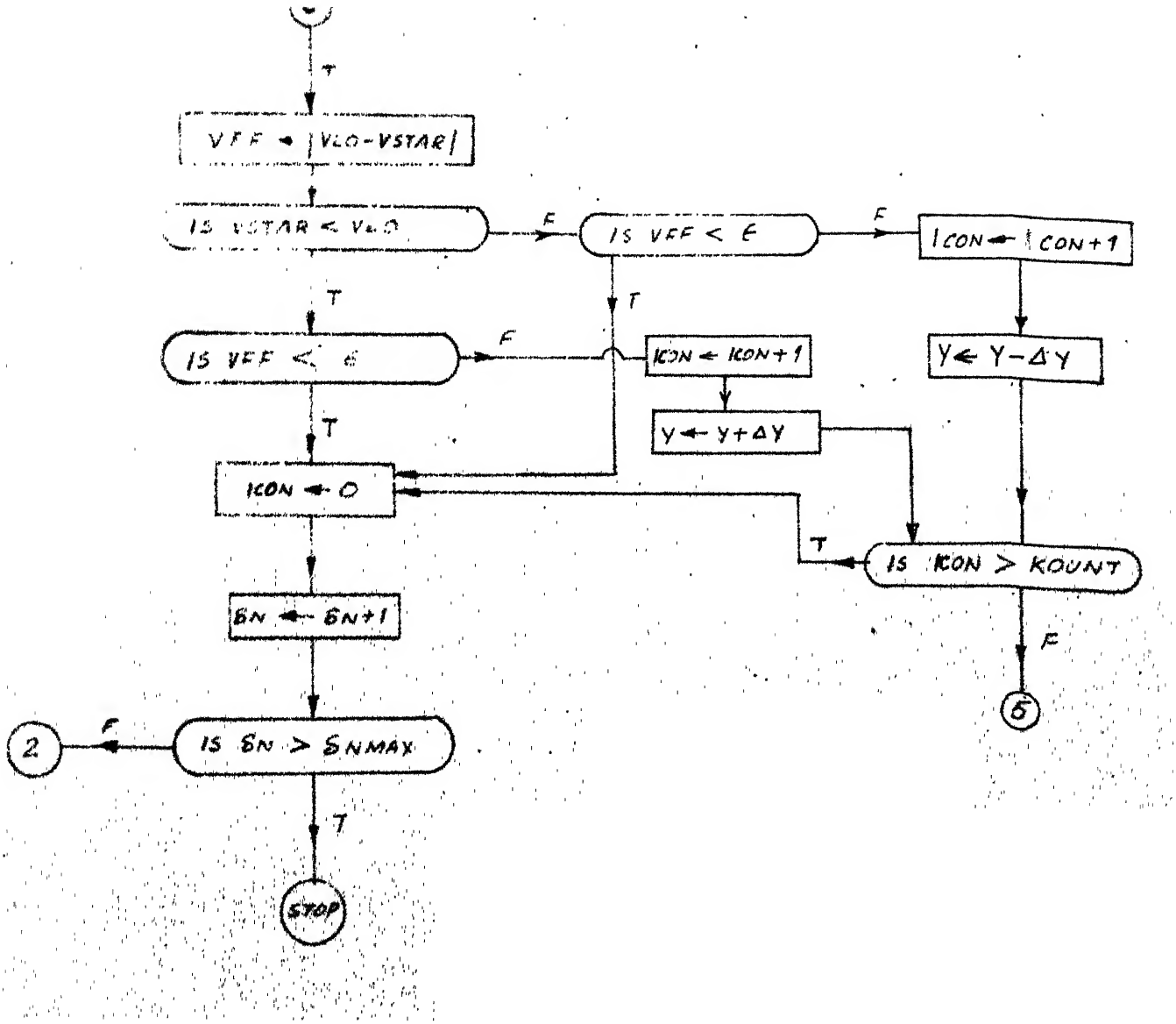
T
VFF ← |VLO-VSTAR|
IS VSTAR < VLO
F
IS VFF < E
F
ICON ← ICON+1
T
T
IS VFF < E
F
ICON ← ICON+1
Y ← Y-ΔY
T
Y ← Y+ΔY
ICON ← 0
T
IS ICON > KOUNT
GN ← GN+1
F
6
2
F
IS GN > GNMAX
T
STOP

```
C**********************************************************
C  -  F  AERONAUTICAL .----THIS PROGRAMME CALCULATES OPTIMUM NOZZLE
C**********************************************************
C  -  S  R.(A)LEAST GROUND DISTANCE FOR TAK--OFF AND FOR LEAST TIM
C     FOR ANY GIVEN AIRCRAFT CONFIGURATION.
      DIMENSION VV  (  ),CTT(2   ),ALPHA(2   ),TT(400),AT(400),ARG(   )
      DIMENSION VEL(4000),ACCN(4000),T(4000),S(4000),ACN(700),AL(700)
      REAL K,M
      COMMON WEIGHT,THETA,TLO,ROC,CLLO,SAREA,TFLEX,ALPHLO,ALPHAG,TROT,
     1ALPHA,CDNOT,ISTAT,AR,E,GNL,AMEW,K
      COMMON A0,B0,SAREA,ROC,ALPHAG,ISTAT,CDNOT,AR,E,GNL,AMEW,CLALPH,CLLO
     1WEIGHT,DELT,DELY
      COMMON ,ALPHLO,TROT,TFLEX,TLO,WEIGHT
      COMMON ,Y  ,N, THETAM,KOUNT,PS
      PRINT 77,ROC,SAREA,CLALPH,ALPHLO,CDNOT,E,AR
      FORMAT(1X,*ROC=*,F9.3,2X,*SAREA=*,F6.1,2X,*CLALPH=*,F4.  ,2X,*ALPHL
     1O=*,F7.4,  X,*CDNOT=*,F5.3,2X,*E=*,F4.1,2X,*AR =*,F4.1)
      COMMON  ,K
      COMMON  ,  ,ISTAT,WEIGHT
      PRINT 1/  X,*K=*,F4.1,5X,*ISTAT=*,F  .1,5X,*WEIGHT=*,F5.1/)
      PRINT
      PRINT
      PRINT  ,*FOR GIVEN RATE OF ROLL IN F.I.*/)
      PRINT
      PRINT  ,*ROLL TIME*,2X,*TIME*,5X,*UPTOROT*,5X,*ROT.*,3X,*TOTAL*,
     1,*VEL*,2X,*VLO*,  X,*ROC*)
      DELT = .
      Y=Y
      CALL FVLO(VLO,ROC)
      CALL ACC(C  ,C11,C12,C13,C14,C15)
      CONTINUE
      T1=  .  50.6
      T  =TSTAT
      ACCN(  )=0
      VEL(  )=ACCN(  )*DELT
      T(  )=  .5
      S(  )=  .
      S(2)=  .5*ACCN(1)*DELT*DELT
      J=2949
      DO 20 J=2,N
      ACCN(J)=C1  -C11*VEL(J)-C12*VEL(J)**2
      VEL(J+1)=VEL(J)++CC5(J)*DELT
      T(J)=T(J-1)+DELT
      S(J+1)=S(J)+(VEL(J)+0.5*ACCN(J)*DELT)*DELT
      VROT=Y*VLO
      TTR=T(J)
      IF(VEL(J+1).GT.VROT) GO TO 21
      SS=S(J+1)
      VELF=VEL(J+1)
      CONTINUE
      N=1
      VVEL(1)=VELF
      CT=C13*ALPHAG-C14*ALPHAG**2-C15
      ACN(1)=C10-C11*VVEL(1)+CT*VVEL(1)**2
      VVEL(2)=VVEL(1)+ACN(1)*DELT
```

```
      )=.,)
 (  )=,.
  (.)=TIM
 T(  )=TT(  )+DELT
 T(I+ )=T(I)+DELT
  TI=TT(I)
 (  )=  .
 L(  )=0.0
 LPHA(  )=AL(I)+ALPHAG
 (I)=T(I-.)+DELT
ALL ALP(A,B,C)
 L(I)=A*T(I)*T(I)+B*T(I)**3+C*T(I)**4
ALPHA(I)=AL(I)+ALPHAG
ARG(I)=PI*(THETA+ALPHA(I))/.9 .
AT(I)=COS(ARG(I))+AMFW*SIN(ARG(I))
CTT(I)=C .*ALPHA(I)-C .4*ALPHA(I)**2-C .
ACN(I)=C *(C .*AT(I)-AMFW*WEIGHT)/WEIGHT-K*C *AT(I)*VV L(I)/WEIGH
Y+C T(I)*VV (I)**2
(I)=(I- )+(VV L(I-.)+ .5*ACN(I-.)*D.LT)*DELT
 (I)- .
 (.)
 (I+.)=VV L(I)+ C.(I)*DELT
  VV (I)
 .
  L
 . . (I) GO TO 2C
 T=T-TAK
 (V IF)
 (  R.LT.VL1) GO TO 35
 (  .LT. PS) GO TO 40
  =ICON+.
 Y=0 LY
 (ICO .GE.KOUNT) GO TO 40
 (V1 .LT. PS) GO TO 40
 .=TI( +)
Y=Y+. LY
 (  .GE.KOUNT) GO TO 4.
  (I)
  C,GAMMA,TGTI,SS,SSR,DISTO,VROT,VLO,ROC
 (I) ,F9.2,2X,F8.1,2X,8(F8.2,2X),F9.2)
 (I=I
 TA=TETA+1.0
 (THETA.GT.TH TAM) GO TO 6
 TO 
 =TIMUL
WEIGHT=WEIGHT+52 .
GO TO 
FORMAT(6F .3.6)
STOP
END
(BATCH SLR)
SUBROUTINE AC(C10,C11,C12,C13,C14,C15)
```

```
      h  IGHT,THETA,TLC,RUC,CLLD,SAREA,TFLUX,ALPHLO,ALPHAG,TROT,
     1 PI,CONST,TSTAT,AR,E,GRAV,AMCW,K
      PI=3.14159
      C1=.5*CD*SAREA*CLALPH*ALPHAG
      C2=.5*CD*SAREA*(CONST+CLALPH*CLALPH*ALPHAG*ALPHAG)/(PI*AR*E)
      C3=.5*CL*SAREA*CLALPH
      C4=.5*CL*SAREA*CLALPH*TSTAT
      C5=.5*CD*SAREA*CLALPH*CLALPH/(PI*AR*E)
      C6=TSTAT
      ARG=(THETA+ALPHAG)*PI/180.
      C7=GRAV*(C5*(COS(ARG)+AMCW*SIN(ARG))-AMCW*WEIGHT)/WEIGHT
      C8=GRAV*K*(COS(ARG)+AMCW*SIN(ARG))/WEIGHT
      C9=GRAV*(C2-AMCW*C3)/WEIGHT
      C10=GRAV*AMCW*C3/WEIGHT
      C11=GRAV*C1/WEIGHT
      C12=GRAV*C2/WEIGHT
      RETURN
      END

      SUBROUTINE DERIV(N,T,Y,DY)
      DIMENSION Y(4),DY(4)
      COMMON /BLK1/ C1,C2,C3,C4,C5,C6,C7,C8,C9,C10,C11,C12
      VLO=Y(1)
      THETA=Y(2)
      RUC=Y(3)
      CLLD=Y(4)
      CALL TFLUX(VLO,RUC)
      COMMON /BLK2/ VLO,THETA,TLO,RUC,CLLD,SAREA,TFLUX,ALPHLO,ALPHAG,TROT,
     1 CONST,TSTAT,AR,E,GRAV,AMCW,K
      ALPHLO=THETA+ALPHAG-ATAN((VLO*SIN(THETA)+RUC)/(VLO*COS(THETA)))
      TROT=ALPHLO*PI/180.
      DIF=TROT-TSTAT
      DENO=C1*CLLD*CLLD
      IF(ABS(DIF).LT.1.E-5) GO TO 1
      DY(1)=(C6+SIN(THETA)-C7*CLLD*CLLD-C8*(TSTAT*SIN(ARG)-WEIGHT))/A
      DY(2)=VLO*(C3*CLLD-C4)/TROT
      DY(3)=VLO*(C5*CLLD*CLLD+C2)/DENO
      DY(4)=(((TSTAT-K*VLO)*COS(ARG)-(C9*ALPHLO*ALPHLO+C4)*VLO*VLO)*VLO*60.
     1/WEIGHT
      RETURN
    1 DY(4)=0.
      RETURN
      END
```

FLOW CHART — CONSTANT SPEED TURNS

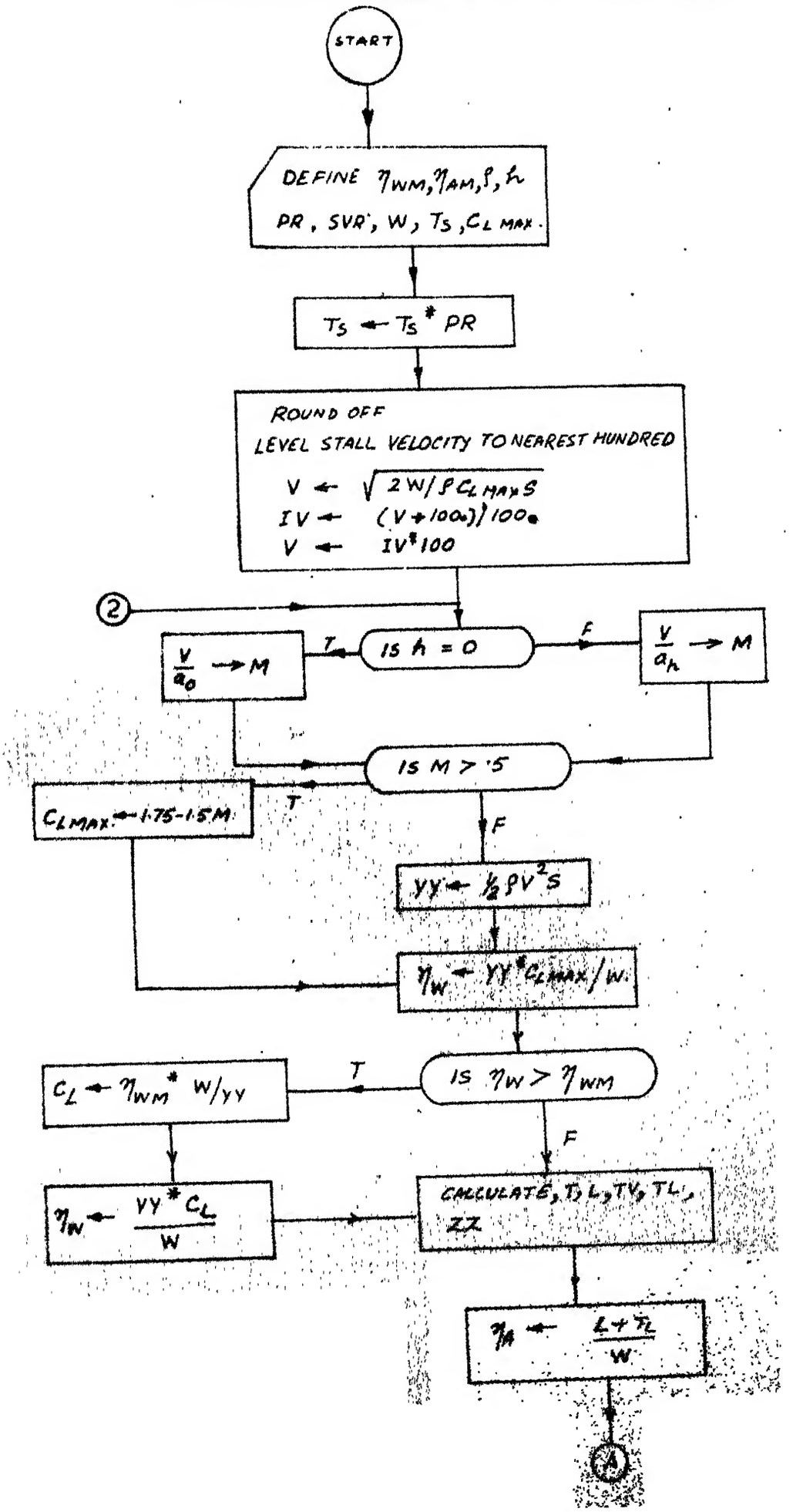

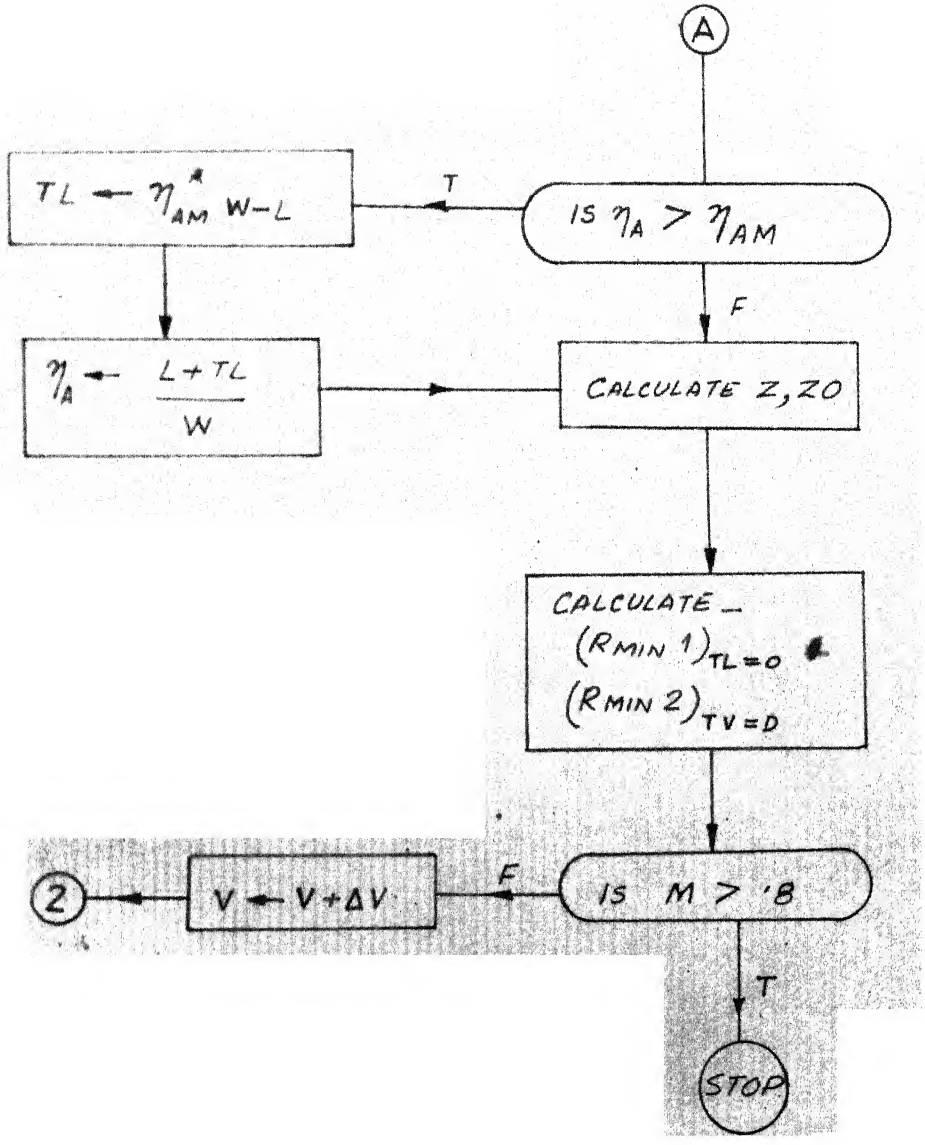
A
IS $\eta_A > \eta_{AM}$
T
$TL \leftarrow \eta^*_{AM} W - L$
F
$\eta_A \leftarrow \frac{L+TL}{W}$
CALCULATE Z, ZO
CALCULATE
$(R_{MIN}\,1)_{TL=0}$
$(R_{MIN}\,2)_{TV=D}$
IS $M > .8$
F
$V \leftarrow V + \Delta V$
2
T
STOP

```
C     ************************************************
C     FORMAT PERFORMANCE---CONSTANT SPEED TURNS---THIS PROGRAMME CALCULA
   TES CONSTANT SPEED LEAST RADIOUS OF TURNS USING VECTORED THRUST AND
      COMPARES IT WITH THE CONVENTIONAL CASE
C     ************************************************
      REAL K,L,NETAW,NETAA,NETAWM,NETAAM,MACHNO
      READ900,SAREA,AR,E,CDNOT,K,GEE
      READ900,TSTAT,CLMAX,AO,SVR,NETAWM,NETAAM,DELV
  900 FORMAT(6F13.6)
      PRINT700,TSTAT,K,SAREA,CDNOT,E,AR,GEE
  700 FORMAT(1X,*TSTAT=*,F8.1,2X,*K=*,F4.1,2X,*SAREA=*,F6.1,2X,*CDNOT=*,
     1F5.2,2X,*E=*,F4.1,2X,*AR=*,F4.1,2X,*GEE=*,F6.2/)
      READ900,W
      READ900,ROE,ALTIFT,NETAWM,NETAAM
      PRINT1000,W,ALTIFT,ROE,NETAWM,NETAAM
      PRINT1100
 1000 FORMAT(10X,*WEIGHT=*,F8.1,2X,*ALTIFT=*,F8.1,2X,*ROE=*,F9.6,2X,*NET
     2AWM=*,F4.1,2X,*NETAAM=*,F4.1/)
 1100 FORMAT(1X,*VELOCITY*,5X,*VKNOTS*,5X,*RMIN FOR DELTAN=0.0*,5X,*RMIN
     2 FOR DELTAN=OPTIMUM*,2X,*MACHNO*,5X,*NETAW*,5X,*NETAA*/)
      PI=4.*ATAN(1.0)
      Y=2.*W/(ROE*CLMAX*SAREA)
      V=SQRT(Y)
      IV=(V+100.)/100.
      V=IV*100
    2 CONTINUE
      VKNOT=V*3600.0/6082.66
      MACHNO=V/(SVR  *AO)
      IF(ALTIFT.EQ.0.0) MACHNO=V/AO
      IF(MACHNO.GT..5) CLMAX=1.75-1.5*MACHNO
      YY=1.6*ROE*V*V*SAREA
      NETAW=YY*CLMAX/W
      IF(NETAW.GT.NETAWM) CLMAX=NETAWM*W/YY
      NETAW=YY*CLMAX/W
      T=TSTAT-K*V
      L=YY*CLMAX
      TV=YY*(CDNOT+(CLMAX**2)/(PI*E*AR))
      ZZ=ARCOS(TV/T)
      TL=T*SIN(ZZ)
      NETAA=(L+TL)/W
      IF(NETAA.GT.NETAAM) TL=NETAAM*W-L
      NETAA=(L+TL)/W
    4 Z=ARSIN(W/(L+TL))
      ZO=ARSIN(W/L)
      RMIN1=((W/GEE)*V*V)/(L*COS(ZO))
      RMIN2=((W/GEE)*V*V)/((L+TL)*COS(Z))
      PRINT800,V,VKNOT,RMIN1,RMIN2,MACHNO,NETAW,NETAA
  800 FORMAT(1X,F7.1,5X,F6.1,10X,F8.1,22X,F8.1,10X,F5.2,5X,2(F5.2,7X))
      V=V+DELV
      IF(MACHNO.GT..8) GO TO 5
      GO TO 2
    5 CONTINUE
      STOP
      END
```

FLOW CHART OPTIMUM TURNS

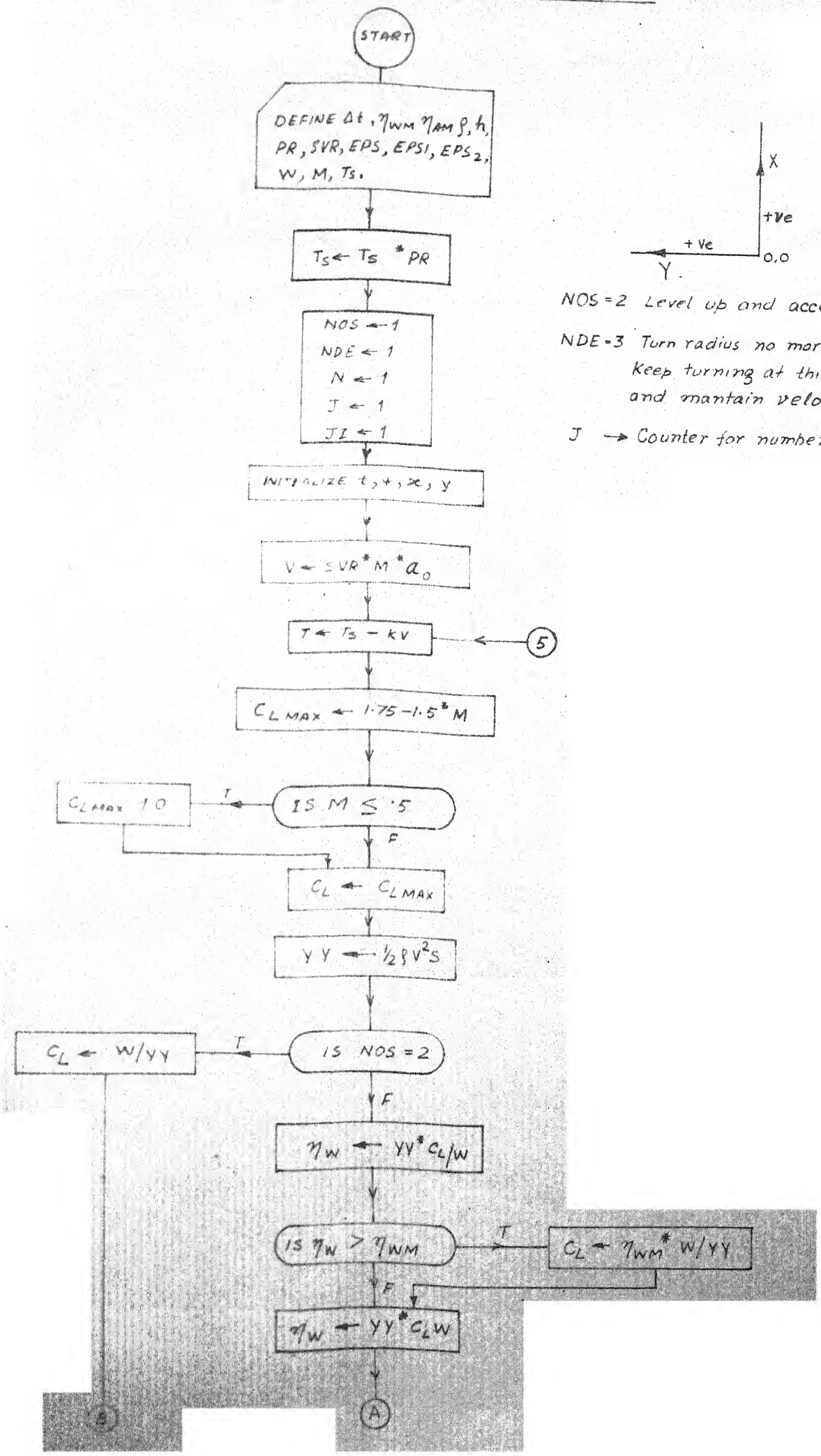

NOS = 2 Level up and accelerat

NDE = 3 Turn radius no more reducing. Keep turning at this radius and mantain velocity

J → Counter for number Of Iterations.

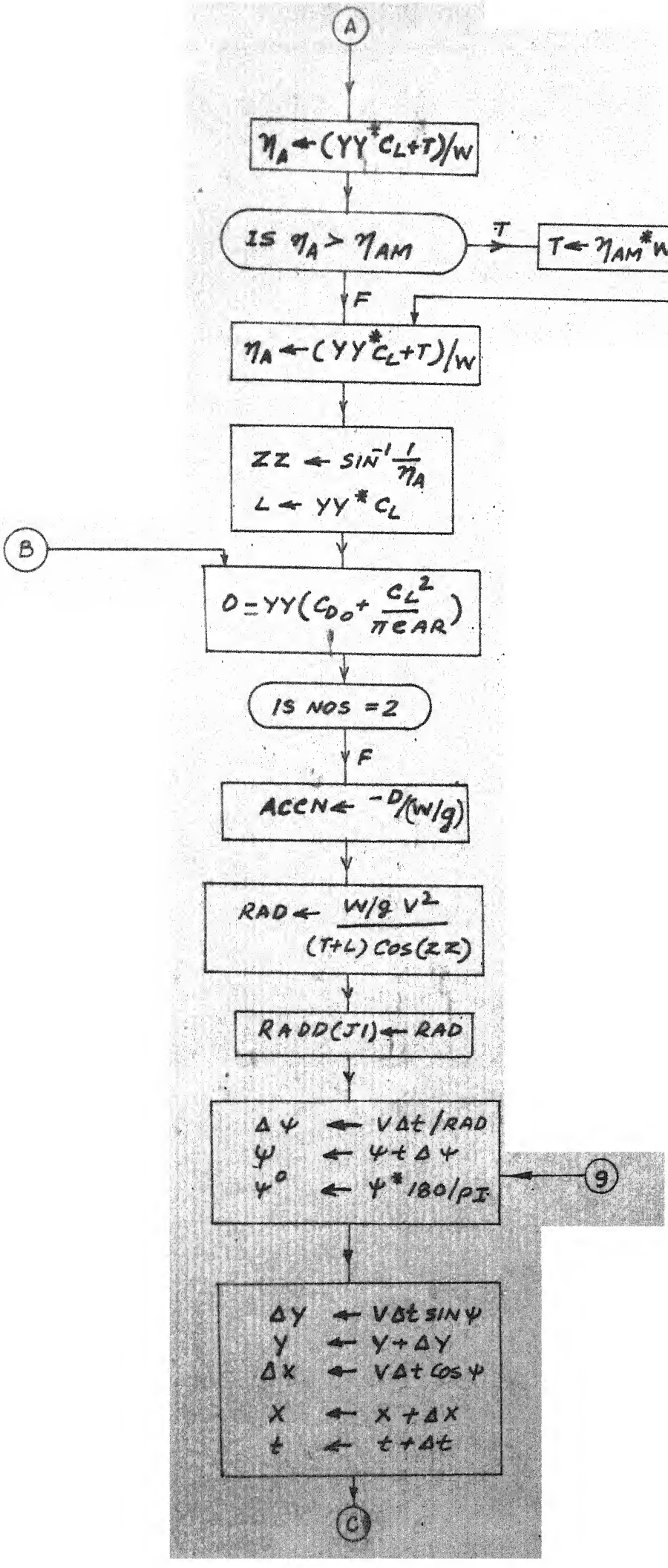
A
$\eta_A \leftarrow (YY^* C_L + T)/W$
IS $\eta_A > \eta_{AM}$
T
$T \leftarrow \eta_{AM}^* W - YY^* C_L$
F
$\eta_A \leftarrow (YY^* C_L + T)/W$
$ZZ \leftarrow \sin^{-1} \frac{1}{\eta_A}$
$L \leftarrow YY^* C_L$
B
$D = YY\left(C_{D_0} + \frac{C_L^2}{\pi e AR}\right)$
IS NOS = 2
F
$ACCN \leftarrow -D/(W/g)$
$RAD \leftarrow \frac{W/g\ V^2}{(T+L)\cos(ZZ)}$
$RADD(J1) \leftarrow RAD$
$\Delta\psi \leftarrow V\Delta t/RAD$
$\psi \leftarrow \psi + \Delta\psi$
$\psi^0 \leftarrow \psi^* 180/PI$
9
$\Delta Y \leftarrow V\Delta t \sin\psi$
$Y \leftarrow Y + \Delta Y$
$\Delta X \leftarrow V\Delta t \cos\psi$
$X \leftarrow X + \Delta X$
$t \leftarrow t + \Delta t$
C

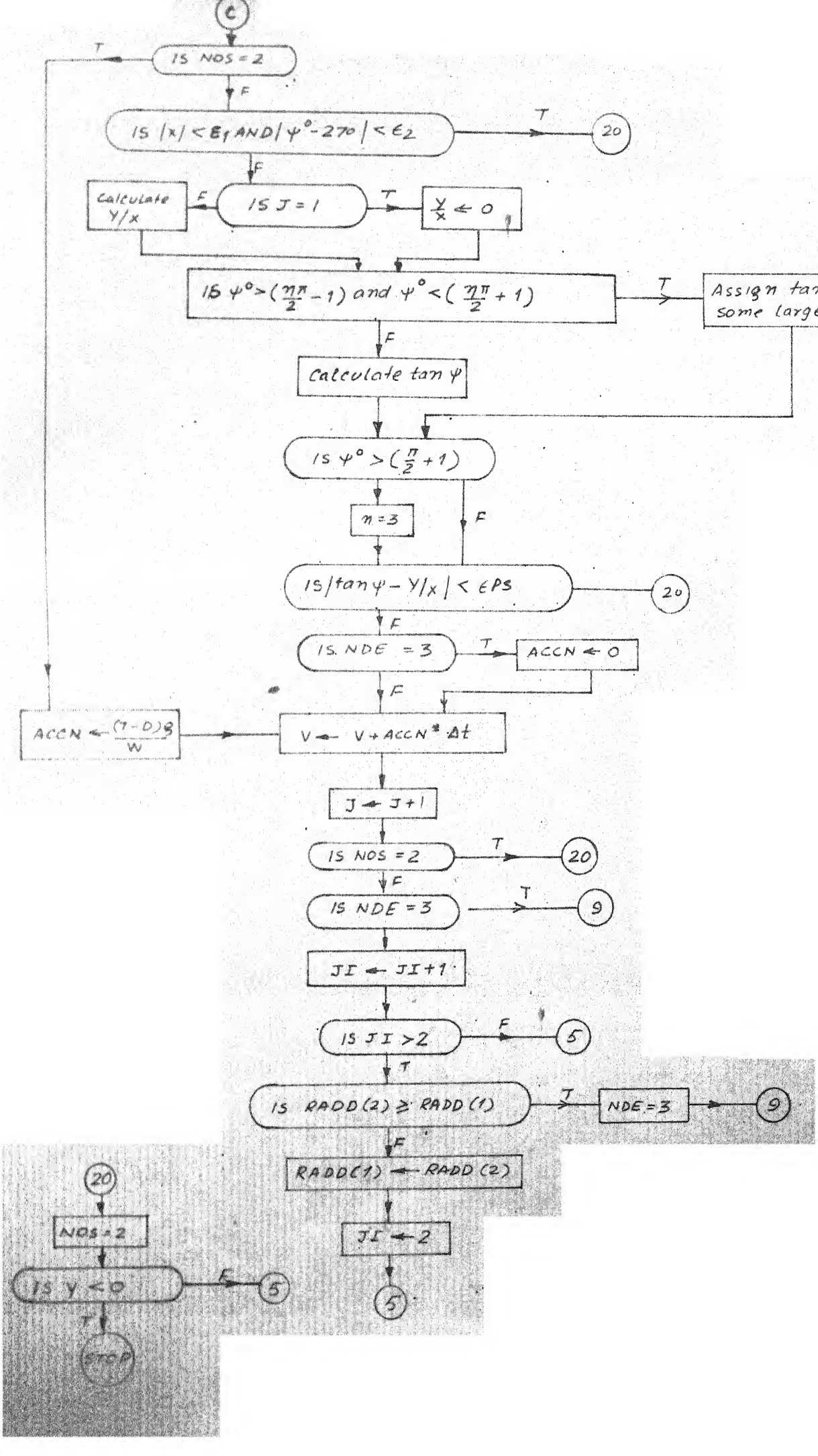
C
IS NOS = 2
T
F
IS |x| < ε1 AND |ψ° - 270| < ε2
T
20
F
Calculate Y/x
F
IS J = 1
T
Y/x ← 0
IS ψ° > (nπ/2 - 1) and ψ° < (nπ/2 + 1)
T
Assign tan ψ some large value
F
Calculate tan ψ
IS ψ° > (π/2 + 1)
n = 3
F
IS |tan ψ - Y/x| < EPS
20
F
IS NDE = 3
T
ACCN ← 0
F
ACCN ← (T - D)g / W
V ← V + ACCN * Δt
J ← J + 1
IS NOS = 2
T
20
F
IS NDE = 3
T
9
JI ← JI + 1
IS JI > 2
F
5
T
IS RADD(2) ≥ RADD(1)
T
NDE = 3
9
F
RADD(1) ← RADD(2)
JI ← 2
5
20
NOS = 2
IS Y < 0
F
5
T
STOP

```
C**********************************************************************
C  MAXIMUM PERFORMANCE----OPTIMUM TURNS---THIS PROGRAMME CALCULATES
C  LEAST POSSIBLE TIME TO COME BACK TO THE TARGET FOR A SECOND PASS
C  WITH THRUST-VECTORING AND COMPARES IT WITH THE CONVENTIONAL CASE
C**********************************************************************
      DIMENSION V(2),ACCN(2),RAD(2),ZAI(2),Y(2),X(2),TIME(2),DEG(2)
      DIMENSION RADD(2)
      REAL K,NETAWM,NETAW,L,MACHNO,NETAA,NETAAM
      READ900,NETAWM,NETAAM
      READ900,DELT
      READ900,ROE,ALTIFT,SVR,PR
      READ900,TSTAT,K,CDNOT,SAREA,AR,E,GEE,AO
      READ900,EPS,EPS1,EPS2
      TSTAT=TSTAT*PR
      READ900,W
      READ900,MACHNO
      PI=4.*ATAN(1.0)
      Y(1)=.0
      NOS=1
      I=1
      T=0.
      L=0.
      D=0.
      WRITE(3,*)
     *,*TSTAT=*,F9.1,2X,*K=*,F4.1,2X,*SAREA=*,F6.1,2X,*CDNOT=*,
     *F6.3,2X,*E=*,F4.1,2X,*AR=*,F4.1,2X,*GEE=*,F6.2/)
      READ900,W,ALTIFT,ROE,NETAWM,NETAAM,SVR,PR
      WRITE(3,1)W,ALTIFT,ROE,NETAWM,NETAAM,SVR,PR
    1 FORMAT(1X,*WEIGHT=*,F8.1,2X,*ALTIFT=*,F8.1,2X,*ROE=*,F9.6,2X,*NET
     *AWM=*,F4.1,2X,*NETAAM=*,F4.1,2X,*SVR=*,F7.4,2X,*PR=*,F7.4/)
      J=1
      J=1
      E
      JJ=1
      V(I)=MACHNO*SVR*AO
      V1=V(I)
      CONTINUE
      T=TSTAT-K*V(I)
      YY=  .5*ROE*V(I)*V(I)*SAREA
      VKNOT=V(I)*3600.0/6082.66
      MACHNO=V(I)/(SVR*AO)
      CLMAX=1.75-.5*MACHNO
      IF(MACHNO.LE..5) CLMAX=1.0
      IF(NOS.EQ.2) CLMAX=W/YY
      IF(NOS.EQ.2) GO TO 17
      NETAA=(YY*CLMAX+T)/W
      IF(NETAA.GT.NETAAM) CLMAX=NETAAM*W/YY
      NETAA=(YY*CLMAX+T)/W
   17 CONTINUE
      L=YY*CLMAX
      D=YY*(CDNOT+(CLMAX**2)/(PI*E*AR))
      ZZ=ARSIN(1.0/NETAA)
      ACCN(I)=-D*GEE/W
      IF(NOS.EQ.2) GO TO 7
      RAD(I)=(W*V(I)*V(I))/(GEE*(T+L)*COS(ZZ))
```

```
      (I)=(G/
     *)*V(I)*V(I)/((T+L)*COS(ZZ))
      IF(
     *.EQ. ) GO TO 14
      WRITE(
     *,V(I),RAD(I),J,NDS,DEG(I),TIME(I),Y(I),X(I),YBYX,TANZAI
     *,*TURNRADIOUS NO MORE REDUCING*/
     *,3X,F6.1,2X,F8.1,2X,F8.1,2X,I2,2
     *,I
     *,F8.2,2X,F8.3,2X,F9.1,2X,F8.1,2X,F9.
     *,2X,F9.3)
      =
      CONTINUE
      IF(J/
     *.NE.J) GO TO 16
      PRINT
     *,V(I),ACCN(I),RAD(I),DEG(I),Y(I),X(I),TIME(I),J,NCS,NDS
     *,YBYX,TANZAI
      CONTINUE
      GO TO 9
      CONTINUE
      DEG(I)=ZAI(I)*180./PI
      IF(NDS.EQ.2) GO TO 1
      IF(NDS.EQ.3) GO TO 22
      PRINT
     *(,V(I),DEG(I),J,NDS,TIME(I),Y(I),X(I),YBYX,TANZAI
     *,*TURNRADIOUS STILL REDUCING BUT IN LINEWITH TARGET SOAC
     *T */
     *(,*VELOCITY*,F6.1,5X,*ZAI*,2X,F7.2,2X,*ITER*,I5,2X,I2,
     *,
     *2X,F
     *.1,2
     *,*Y*,F8.1,2X,*X*,F8.1,2X,*YBYX*,F9.2,2X,*TANZAI*,
     *F
     */)
      GO TO
      IF(J/
     *.NE.J) GO TO 3
      PRINT
     *,V(I),ACCN(I),RAD(I),DEG(I),Y(I),X(I),TIME(I),J,NCS,NDS
     *,YBYX,TANZAI
      GO TO
      IF(
     *.EQ.2) GO TO 5
      IF(
     *.EQ.3) GO TO 6
      PRINT
     *,V(I),DEG(I),J,NDS,TIME(I),Y(I),X(I),YBYX,TANZAI
      FORMAT(
     *,*IN LINE WITH TARGET.COMMENCING LEVEL PULL-OUT
     */
     *,*VELOCITY*,F6.1,5X,*ZAI*,2X,F7.2,2X,*ITER*,I5,2X,I2,2X,F6.
     *,
     *,F8.1,2X,F8.1,2X,F9.3,2X,F9.3/)
      GO TO
      IF(Y(
     *).LT.
     *.0) GO TO 3
      CONTINUE
      PRINT
     *,V(I),ACCN(I),RAD(I),DEG(I),Y(I),X(I),TIME(I)
      FORMAT(1X,
     *,*FINAL VALUES ARE AS BELOW*/1X,F6.1,2X,F6.1,2X,F8.1,2X,F
     *,
     *,F8.1,2X,F8.1,2X,F8.3)
      STOP
```

REFERENCES

1. Lean, D., A discussion of some jet lift V/STOL aircraft-Characteristics and their likely effects on operational applications, RAE Technical Report 66150 (ARC CP 1082) (1966).

2. Illing Worth, J.K.B., Shayler, J.S., Blind flying of V/STOL aircraft with particular reference to take-off and landing, Symposium on V/STOL aircraft AGARD, Paris, June 1960 (ARC 22427).

3. King, K.P., McPherson, A., A piloted simulator study of a jet VTOL aircraft in partially jet borne flight, RAE Technical Report 68301 (ARC 31163) (1968).

4. Passt, O.E., VTOL aircraft development, Journal of R.A.S., July 1967, p 489.

5. David, A. Brown, Vectored Thrust Manoeuvrability explored, A.W. and S.T., December 13, 1971, p 36.

6. J.F. Farley, Piloting aspects of jet V/STOL, The Aeronautical Journal, October 1968, p 893.

7. R.D. Hiscocks, V/STOL aircraft - A perspective, The Aeronautical Journal, Jan. 1968, p. 11.

8. M. Flemming, Aspects of Do-31 jet lift V/STOL aircraft, The Aeronautical Journal, Aug. 1968, p. 719.

9. E. Huntley, Optimal paths for minimum landing transition distance for jet lift V/STOL aircraft, The Aeronautical Journal, May 1972, p.308.

10. M.J. Brennan, V/STOL developments in Hawker Siddeley Aviation Limited, The Aeronautical Journal, June, 1972, p. 391.

11. Kuhn, R.E., Review of basic principles of V/STOL aerodynamics, NASA, TN D-731 (1961).

12. H.L. Braasch, R.A. Fuhrman, George D. Ray, Development of V/STOL jet aircraft, Proceedings of the Naval Aviation meeting published by the Institute of Aeronautical Sciences, New York, Aug. 1957, p.62-70

13. Campbell, John Paul, Vertical take-off and landing aircraft.

REFERENCES (Contd.)

14. Barnes W. McCormick, Aerodynamics of V/STOL Flight.

15. C. Ming Wong, VTOL Vehicles: Practice and Potential.

16. Davidson, C, Aeroplane performance theory for pilots and flight engineers.

17. Mises, Richard, Von, Theory of flight.

18. Schutt, Karl, Elements of Aeronautics.

19. F.G. Swanborough, Vertical flight aircrafts of the World.

20. Angelo Miek, Flight Mechanics Vol. 1.

21. Perkins and Hage, Aeroplane performance, stability and control.

22. Harrier Study - Flight International, Feb.17, 1972, p. 276.

23. German jet VTOL Expertise - A.W. and S.T., April 24, 1972, p.107.

24. Harrier Flexibility - A.W. and S.T., July 5, 1972, p. 52.

25. Harrier Programme for Broad VTOL Data - A.W. and S.T., Oct. 25, 1971, p. 47.

26. Harrier Fitted to Marine Tactics - A.W. and S.T., Oct. 18, 1971, p. 38.

27. Harrier Suited to NATO Role - A.W. and S.T., Jan. 4, 1971, p. 13.

28. Harriers - U.S. Navy Choice for sea control - A.W. and S.T., May 8, 1972, p. 23.